Key message: Copper deficiency and excess differentially affect iron homeostasis in rice and overexpression of the *Arabidopsis* high-affinity copper transporter *COPT1* slightly increases endogenous iron concentration in rice grains.

Authors: Amparo Andrés-Bordería[1,2], Fernando Andrés[3+], Antoni Garcia-Molina[1]*, Ana Perea-García[1#], Concha Domingo[3], Sergi Puig[1#] and Lola Peñarrubia[1,2]

Title: Copper and ectopic expression of the Arabidopsis transport protein COPT1 alter iron homeostasis in rice (*Oryza sativa* L.)

[1]Departamento de Bioquímica y Biología Molecular. Facultad de Ciencias Biológicas. Universitat de València. Dr Moliner 50. 46100 Burjassot, Valencia, Spain.

[2]Estructura de Recerca Interdisciplinar en Biotecnologia i Biomedicina (ERI BIOTECMED), Universitat de València. Dr Moliner 50. 46100 Burjassot, Valencia, Spain.

[3]Instituto Valenciano de Investigaciones Agrarias. Carretera Moncada - Náquera Km 4.5 Moncada 46113 – ES Valencia, Spain.

[+]Present address: INRA, UMR AGAP, Equipe Architecture et Fonctionnement des Espèces Fruitières, Avenue d'Agropolis - TA-A-108/03, 34398 Montpellier Cedex 5, France.

*Present address: Department Biology I. Plant Molecular Biology (Botany). Ludwig Maximilian University Munich, Großhaderner Str. 2–4. D-82152. Planegg-Martinsried, Germany.

#Present address: Departamento de Biotecnología. Instituto de Agroquímica y Tecnología de Alimentos (IATA). Agencia Estatal Consejo Superior de Investigaciones Científicas (CSIC). Calle Catedrático Agustín Escardino 7, Paterna 46980 (Valencia) Spain.

Corresponding author: Dr. L. Peñarrubia, Departamento de Bioquímica y Biología Molecular. Facultad de Ciencias Biológicas. Universitat de València. Avda. Dr. Moliner, 50. 46100-Burjassot, Valencia, Spain. Phone: +34-963543013; Fax: +34-963544635; E-mail: lola.penarrubia@uv.es

Abstract

Higher plants have developed sophisticated mechanisms to efficiently acquire and use micronutrients such as copper and iron. However, the molecular mechanisms underlying the interaction between both metals remain poorly understood. In the present work, we study the effects produced on iron homeostasis by a wide range of copper concentrations in the growth media and by altered copper transport in *Oryza sativa* plants. Gene expression profiles in rice seedlings grown under copper excess show an altered expression of genes involved in iron homeostasis compared to standard control conditions. Thus, ferritin *OsFER2* and ferredoxin *OsFd1* mRNAs are down-regulated whereas the transcriptional iron regulator *OsIRO2* and the

nicotianamine synthase *OsNAS2* mRNAs rise under copper excess. As expected, the expression of *OsCOPT1*, which encodes a high-affinity copper transport protein, as well as other copper-deficiency markers are down-regulated by copper. Furthermore, we show that *Arabidopsis COPT1* overexpression ($C1^{OE}$) in rice causes root shortening in high copper conditions and under iron deficiency. $C1^{OE}$ rice plants modify the expression of the putative iron-sensing factors *OsHRZ1 and OsHRZ2* and enhance the expression of *OsIRO2* under copper excess, which suggests a role of copper transport in iron signaling. Importantly, the $C1^{OE}$ rice plants grown on soil contain higher endogenous iron concentration than wild-type plants in both brown and white grains. Collectively, these results highlight the effects of rice copper status on iron homeostasis, which should be considered to obtain crops with optimized nutrient concentrations in edible parts.

Key words: copper; iron; metal transport; *Oryza sativa*; COPT1; OsIRO2

Acknowledgments: This work has been supported by grants BIO2011-24848 and BIO2014-56298-P from the Spanish Ministry of Economy and Competitiveness, and by FEDER funds from the European Union. We acknowledge Àngela Carrió-Seguí (Universitat de València) and Kiranmayee Pamidimukkala for their technical help with this manuscript**.** We also acknowledge the *Servei Central d'Instrumentació Científica* (*Universitat Jaume I*) and SCSIE (*Universitat de València*) for the ICP-MS and atomic absorption spectrophotometry determinations and greenhouse facilities.

Conflict of Interest: The authors declare that they have no conflict of interest.

Author Contributions Statement: CD, SP and LP conceived the idea and wrote the manuscript. AA-B, FA and CD perform the rice microarray and transformation experiments. AA-B, AG-M and AP-G perform the physiological and molecular experiments in rice plants.

Introduction

Numerous interactions between copper (Cu) and iron (Fe) homeostasis have been described in *Saccharomyces cerevisiae* (Puig and Thiele 2002), humans (Gulec and Collins 2014) and plants (Puig et al. 2007). Cu and Fe are essential transition metals for living organisms. Both elements have an electronic configuration that allows them to form coordination complexes with organic molecules and to act as redox cofactors in many proteins, being key components in respiratory and photosynthetic electronic transport chains (Puig and Peñarrubia 2009; Yruela 2013). For instance, Fe serves as a cofactor for several proteins in chloroplasts, including ferredoxin (*Fd*), which is involved in the electron transport chain (Briat 1996). Cu and Fe display similar physical and chemical properties, and changes in their bioavailability during atmosphere evolution have driven metalloprotein substitution (Crichton and Pierre 2001). Fe uptake and mobilization depend on Cu in yeast and humans (Gulec and Collins 2014), although this connection remains needs in depth investigation in plants (Bernal et al. 2012; Waters et al. 2012; Perea-García et al. 2013; Waters and Armbrust 2013). Under metal deficiency conditions, induction of reactive oxygen species (ROS) could also affect Cu-Fe interactions (Ravet and Pilon 2013). Mechanisms of excess metal detoxification include the synthesis of metallothioneins (MTs), which contain cysteine-rich domains with the capacity to interact with metals (Leszczyszyn et al. 2013).

Cu enters the plant through members of the CTR family of high-affinity Cu transport proteins, denoted as COPT in plants. The CTR/COPT protein family is conserved in eukaryotes and functions in Cu^{+} uptake (Puig 2014). These proteins

contain three transmembrane segments with the amino-terminus in the extracytosolic space and the carboxyl-terminus facing the cytosol. Most CTR-type proteins contain methionine-rich domains at their amino-terminus that form Cu-binding centers. *Arabidopsis* contains six COPT genes, annotated as *COPT1-6* (Sancenón et al. 2003; Puig 2014; Peñarrubia et al. 2015), whereas *Oryza sativa* expresses seven COPT family members listed as *OsCOPT1-7* (Yuan *et al.*, 2010, 2011). Transgenic *Arabidopsis* lines that overexpress the *AtCOPT1* transport protein ($COPT1^{OE}$ or $C1^{OE}$) are Cu sensitive (Andrés-Colás et al. 2010), whereas *Arabidopsis copt2* mutants, which lack of *COPT2* expression, exhibit resistance to Fe deficiency (Perea-García et al. 2013). Specifically, the *copt2* lines exhibit reduced chlorosis and produce a larger number of seeds under simultaneous Cu and Fe deficiencies, which supports the interaction between both metals (Perea-García et al. 2013).

Fe deficiency, which leads to anemia, is a widespread health problem that affects more than 2 billion people worldwide (White and Broadley 2009; Stevens et al. 2013). Multiple interventions have been encouraged to reduce micronutrient malnutrition, and genetic engineering-based biofortification is one of the most effective. Since rice (*Oryza sativa*, L.) is one of the most widely consumed crops worldwide, biofortification strategies for increased Fe transport and delivery to rice grains have been prioritized as a suitable approach to provide Fe to anemia-susceptible populations (Sperotto et al. 2012; Bhullar and Gruissem 2013).

Nutrient uptake and distribution in plants depend on many processes, which makes difficult the use of conventional breeding techniques to improve crop nutritional quality. Unlike other grass species, rice utilizes strategy II and partially

strategy I to transport Fe (Ishimaru et al. 2006). Strategy I consists in proton excretion, ferric-chelate reduction, and Fe uptake through IRON REGULATED TRANSPORTER (IRT1). A lack of inducible ferric-chelate reductase activity at the root surface has been described in rice (Ishimaru et al. 2006). In Strategy II, Fe(III)-phytosiderophore chelates of the mugineic acid family (MAs) are synthesized from *S*-adenosylmethionine (SAM) through nicotianamine (NA), an intermediate produced, among others, by NA synthase (NAS) and NA aminotransferase (NAAT) enzymes. Although originally identified as Fe(III)-phytosiderophore transporters, some of the members of the yellow-stripe (YS1/YSL) family transport structurally similar compounds, such as Fe(II)-NA. In this sense, the rice OsYSL2 member of this family transports Fe(II)- and Mn(II)-NA, but not Fe(III)-deoxymugineic acid (Koike et al. 2004). *OsYSL2* expression also leads to higher Fe concentration in seeds (Ishimaru et al. 2010). A successful strategy has consisted in increasing Fe transport to the aerial part through NA synthesis, which acts as an Fe chelator in the phloem by overexpressing NAS genes (Lee et al. 2009; Johnson et al. 2011). Plastidic Fe storage protein ferritin, which aimed to prevent cell damage caused by the free metal, was specifically expressed in the endosperm leading to increased Fe concentration in rice grains (Goto et al. 1999; Oliva et al. 2014).

The distinct networks that regulate Fe sensing, uptake and intracellular distribution in rice are being uncovered (Kobayashi and Nishizawa 2012). Two candidates of putative Fe-sensing factors have been described in rice: IRON DEFICIENCY-RESPONSIVE ELEMENT–BINDING FACTOR 1 (OsIDEF1) and HEMERYTHRIN MOTIF-CONTAINING REALLY INTERESTING NEW GENE- AND ZINC-FINGER (OsHRZ) proteins (Kobayashi and Nishizawa 2014). OsIDEF1, whose transcript levels do not

change in response to Fe availability, is a positive regulator of *IRON-RELATED TRANSCRIPTION FACTOR 2* (*OsIRO2*), a member of the basic helix-loop-helix (bHLH) transcription factor family induced under Fe deficiency (Ogo et al. 2006). Rice lines overexpressing *OsIRO2* exhibit improved tolerance to Fe deficiency, which indicates that OsIRO2 plays a key role in Fe uptake and transport in both germination and seed development (Ogo et al. 2011). OsHRZ1 and OsHRZ2 are E3 ubiquitin ligases that negatively regulate Fe accumulation under Fe sufficiency. However, the nature of the detected Fe signal, which may involve other metals, oxygen or redox status, remains elusive (Kobayashi et al. 2013; Kobayashi and Nishizawa 2014).

The present work aims to explore the interaction between the homeostatic networks of Cu and Fe in a relevant crop like rice. In order to explore new Fe and Cu homeostatic connections, we analyze the expression of Fe-related genes when adding or not Cu to the media and in transgenic rice plants that overexpress *AtCOPT1*.

Material and Methods

Plant growth conditions and treatments

Rice (*O. sativa* L. cv. Nipponbare) seeds were surface-sterilized and stratified for 2 days at 4°C, and then germinated on ½ MS (Sigma) plates with 1% sucrose (Murashige and Skoog 1962) considered as the standard commercial control condition. Variable $CuSO_4$ concentrations were added whenever indicated. For severe Cu-deficient conditions, ½ MS was supplemented with 100 µM bathocuproinedisulfonic acid disodium (BCS). In order to test the effect of Cu and Fe deficiency on plants, the

components of ½ MS were prepared separately according to the following conditions: macronutrients (10 mM NH_4NO_3, 9.4 mM KNO_3, 0.37 mM $MgSO_4$, 0.62 mM KH_2PO_4, and 1.13 mM $CaCl_2$), micronutrients (50 μM H_3BO_3, 36.6 μM $MnSO_4$, 15 μM $ZnSO_4$, 0.57 μM $NaMoO_4$, and 0.05 μM $CoCl_2$), 50 μM Fe-EDTA, 0.25 mM KI, 1 μM $CuSO_4$, 0.05% MES, 1% sucrose, and 0.8% phytoagar, pH 5.7. The plates prepared as specified were considered as Fe- and Cu-sufficient medium (+Cu +Fe). The rest of the media were prepared as follows: Cu-deficient (with no added Cu) and Fe-sufficient medium (-Cu +Fe), Cu-sufficient and Fe-deficient (with no added Fe) medium (+Cu -Fe), and Cu and Fe -deficient (with no added Cu and Fe) medium (-Cu -Fe). Seedlings were grown under neutral day photoperiod (12 h light, 23°C / 12 h darkness, 16°C) (65 mmol m^{-2} cool-white fluorescent light) in a Sanyo Growth Cabinet MLR-350T for 8 days.

For hydroponic cultures, rice grains were germinated in Petri dishes filled with deionized water at 30° C in darkness. Then plantlets were cultivated in hydroponic boxes that contained standard Hoagland solution (0.1 X) pH 5.8, as described by Hermans et al. (2005). After 2 weeks of adaptation, the -Cu -Fe treatment (corresponding to Hoagland medium without Cu and Fe) applied, for 2 more weeks. For these experiments, plants were grown under long day conditions (16 h light, 23°C / 8 h darkness, 16°C) (65 mmol m^{-2} cool-white fluorescent light) for 1 month.

The obtained 5 month-old plants, unless other age is stated, were grown in the greenhouse in 22 x 20 cm pots that contained a 3:1 mixture of substrate (SEED PRO5050 Projar Professional) and perlite (pH 6-6.5). Plants were grown under long day conditions (16 h light, 23°C / 8 h dark, 27°C). Relative humidity was maintained

between 65-83% until the emergence of 6-7 leaves in panicles. Root and shoot lengths from 8 day-old seedlings were measured by the Image J (http://rsb.info.nih.gov./ij) software.

Chlorophyll quantification

Chlorophylls from the excised rice aerials parts were extracted with cold acetone 90% (v/v) and gentle agitation at 4°C overnight. Subsequently, chlorophyll concentration was spectrophotometrically determined as described in Garcia-Molina et al. (2011), and the resulting values were normalized to fresh weight (F.W.).

Rice transformation

The expression cassette *CaMV35S::AtCOPT1-HA::NOS* (Andrés-Colás et al. 2010) was excised from the pBI121 plasmid by *HindIII* and *SacI* digestion and was cloned into a *pCAMBIA1305.1* binary vector (Cambia, http://www.cambia.org/). The resulting plasmid was transformed into the *Agrobacterium tumefaciens* C58 strain. Rice (*O. sativa* L. cv. Nipponbare) plants were transformed according to Hiei et al. (1994).

Gene expression by semi-quantitative and real-time quantitative PCR

Total RNA was extracted from 8 day-old seedling shoots grown under the indicated conditions by the RNAeasy mini plant kit (Qiagen) following the manufacturer's instructions. RNA was quantified by UV spectrophotometry and its integrity was visually assessed on ethidium bromide-stained agarose gels. Total RNA (1.5 µg) was first converted into cDNA by reverse transcription using SuperScript II

reverse transcriptase (Invitrogen) and anchored oligo(dT)$_{15}$ (Roche). Semi-quantitative PCRs were performed with specific primers (Supplemental Table S1). Real-time quantitative PCRs were carried out with SYBR Green qPCR SuperMix-UDG with ROX (Invitrogen) and a specific primer (Supplemental Table S1) in a CFX96 Touch Real-Time PCR Detection System (Bio-Rad) with one cycle of 95°C for 2 min, and 40 cycles that consisted in 95°C for 30 s and 60°C for 30 s. Values were normalized to the *ACTIN1* mRNA levels, and the wild-type (WT) used under the control conditions was taken as a reference.

Gene expression analysis by long oligonucleotide microarrays

Genome-wide gene expression studies were carried out by rice 45 K whole-genome oligonucleotide DNA microarrays, provided by the University of Arizona (http://www.ag.arizona.edu/microarray). The RNA from four independent biological replicates of 8 day-old seedling shoots grown under each condition (½ MS and ½ MS + 75 µM $CuSO_4$) was amplified by the MessageAmp aRNA kit (Ambion). The obtained amplified RNA (aRNA) was labeled by using the CyDye Post-Labeling Reactive Dye Pack, which generates fluorescent Cy3- and Cy5-labeled probes by a post-labeling (amino allyl) method (GE Healthcare). Each biological replicate was labeled with Cy3 and Cy5 to produce four pairs of replicate dye-swaps, which were used for microarray hybridization. Both amplified RNA and labeled aRNA were quantified in a NanoDrop ND-1000 spectrophotometer (Thermo scientific). Manual hybridization was performed according to the following protocol: microarrays were re-hydrated by exposing them to water vapor for 10 s (four times). Next microarrays were cross-linked by ultraviolet

(UV) irradiation of 180 mJ in a Stratalinker 1800 UV (Stratagene). Subsequently, microarrays were washed with 1% sodium dodecyl sulfate (SDS) (w/v) for 5 min and 10 times with H_2O milliQ (Millipore), washed with 100% ethanol 5 times and then dried by centrifugation at 200 g. After this pre-treatment, microarrays were hybridized overnight at 55°C with hybridization solution [48 pmol of each labeled sample; deionized formamide 50% (v/v)] 3 X saline-sodium citrate (SSC); Denhardt´s solution [5 X and SDS 0.1% (w/v)]. The hybridization solution was denaturalized for 5 min at 65°C and applied between the microarray and a coverslip LifterSlipTM (Erie Scientific). After hybridization, microarrays were washed with SSC and SDS at decreasing concentrations and dried by centrifugation at 1000 rpm. The hybridized microarrays were scanned using a Gene Pix Autoloader 4200AL (Axon/Molecular Devices) at 532 nm (Cy3) and 635 nm (Cy5). The expression values were obtained with the *GenePix Pro 6.0 microarray-analysis* software (Axon Molecular Devices). Quality control, normalization and determination of the differentially expressed genes were conducted in R using the Limma package (Smyth 2005), as previously described in (Andrés et al. 2009). To determine the false-positive ratio (FDR), the P-values were adjusted by a multiple test according to the Benjamini and Hochberg (1995) method. Genes that displayed a differential expression with fold-change (FC) minimum of 2 for both conditions, represented as $\log_2(FC) \geq |1|$ (-1 > log-fold change [½ MS + 75 µM/ ½ MS] > 1) with a P-value of 0.05 (FDR = 0.5%) were selected. The microarray datasets have been deposited in the public NCBI database (GSE8910).

Western Blot

Crude extracts from the WT and transgenic lines grown on 75 µM $CuSO_4$ were obtained by crushing the material in a mortar with N_2 liquid and adding 3 X SDS buffer [Tris-HCl 250 mM, pH 6.8; glycerol 20% (v/v); SDS 4% (w/v); β-mercaptoethanol 10% (v/v) and bromophenol blue 0.025% (w/v)] in a 1:2 ratio (w/v). Samples were boiled for 30 min at 90°C and centrifuged at 12000 rpm at 4°C for 30 min to remove cell debris. Twenty µl of the protein extract were analyzed by SDS-PAGE, transferred to a nitrocellulose membrane and blotted with an antibody against Human Influenza Hemaglutinin epitope (HA) (Roche). Ponceau staining was used as a loading control. Antigen/antibody-peroxidase detection was carried out with the ECL system (Amersham) following the manufacturer's recommendations and exposing the membrane in an ImageQuant 4000 instrument (GE Healthcare).

Metal accumulation and hormone measurements

For the biochemical analyses, fresh 8 day-old *O. sativa* seedling shoots grown under the indicated conditions were washed once with 20 µM EDTA and 3 times with MilliQ water. For the ABA, IAA and JA determinations, plant material was lyophilized and then analyzed by UHPLC (ultra-high-pressure liquid chromatography) (Q-Exactive, ThermoFisher Scientific) at the IBMCP (Valencia, Spain). Lyophilized samples and seedlings were digested with 65% (v/v) HNO_3 at 80 to 90°C. Digested samples were diluted with Millipore water (Purelab Ultra), and Cu and Fe concentrations were determined by inductively coupled plasma mass spectrometry (ICP-MS) at the *Servei Central d'Instrumentació Científica* (Universitat Jaume I) and *Servei Central de Suport a la Investigació Experimental* (SCSIE) (Universitat de València).

Perl´s Staining

Seeds from the WT and transgenic plants were germinated in ½MS and embedded with equal volumes of 4% (v/v) HCl and 4% (w/v) K-ferrocyanide (Perl´s stain solution) for 15 min and incubated for 30 min at room temperature (Stacey et al. 2007).

Statistical analysis

A statistical analysis of the relative expression studies was performed by comparing the relative expression of the genes based on the pair-wise fixed reallocation randomization test ($P < 0.05$; (Pfaffl 2001)). For the remaining parameters, this was carried out by a two-way ANOVA with the means compared by the Duncan test ($P < 0.05$), or by a Kruskal-Wallis test when the data distribution was non parametric, using the InfoStat software, version 2010 (http://www.infostat.com.ar) (Di Rienzo et al. 2011).

Results

Characterization of copper nutritional responses in *Oryza sativa*

To evaluate how rice Cu status changes in accordance with the Cu present in the medium, 8 day-old seedlings were grown on ½ MS commercial plates supplemented with Cu at concentrations between 0 and 100 μM (Figure 1a). As expected, we observed a positive correlation between the endogenous Cu concentration found in shoots from 8 day-old seedlings and the increasing of Cu added

to the medium. According to the Cu sufficiency range established for higher plants (5–20 μg/g DW) (Marschner 2012), the shoots of rice seedlings grown in medium with no Cu supplementation (0 μM $CuSO_4$) contained Cu levels at the lower limit of sufficiency (5.1 μg/g DW), whereas Cu excess was found in plants grown on the media supplemented with concentrations of 10 μM $CuSO_4$ (28.6 μg/g DW) and higher (Figure 1a).

The physiological toxic effect of Cu in rice seedlings was demonstrated as root growth inhibition. Cu led to a significant reduction in root length, with a 50% reduction in the medium supplemented with 50 μM $CuSO_4$ (Figure 1b). A similar trend has been previously observed in *Arabidopsis* (Andrés-Colás et al. 2010). Cu supply did not impact on the phytohormones abscisic acid (ABA) and jasmonate (JA) content in shoots (Figure S1). However, auxins (IAA) concentrations in shoots analyzed in a Cu deficiency medium, obtained by adding a Cu chelator (Cu deficiency: 0 μM $CuSO_4$ + 100 μM BCS) or in Cu excess (10 μM $CuSO_4$) revealed significant differences, with decreased levels under Cu excess (Figure 1c).

Since plasma membrane high-affinity Cu transport proteins are well-recognized as Cu deficiency markers in *Arabidopsis* (Yamasaki et al. 2009; Bernal et al. 2012; Andrés-Colás et al. 2013), the *OsCOPT1* (LOC_Os01g56420) transcript level was determined by quantitative RT-PCR in the rice seedlings grown under the aforementioned wide range of Cu conditions. The *OsCOPT1* transcript levels were high at 0 μM $CuSO_4$ and dropped dramatically when the medium was supplemented with Cu (Figure 2). Conversely, the transcript levels of metallotionein *OsMT1c* (LOC_Os12g38010), which is considered a Cu-excess marker in *Arabidopsis* (Andrés-

Colás et al. 2013), raised in the seedlings cultivated on the media that contained more than 10 μM $CuSO_4$ (Figure 2). This trend agreed with the endogenous Cu concentration variation (Figure 1a) and further supported that 10 μM $CuSO_4$ can be considered a Cu excess medium. However, for 0 μM $CuSO_4$, plants underwent slight Cu deficiency at the molecular level by expressing the high-affinity Cu transport protein *OsCOPT1*.

Thus, we established Cu nutritional ranges for rice seedlings under our experimental conditions based on metal concentration, physiologic parameters and molecular responses, which reflect the endogenous cellular metal status.

Transcriptomic profile unveils an influence of copper on iron homeostasis

To gain further insight into the molecular responses affected by the Cu nutritional status, 8 day-old *O. sativa* seedling shoots were used to perform a global gene expression analysis by DNA microarrays. Two different Cu concentration conditions were compared, ½ MS standard commercial control (no Cu added; 0 μM $CuSO_4$) and Cu excess (75 μM $CuSO_4$), as the latter has been shown to affect root length and metal concentration, and practically eliminates *OsCOPT1* expression (Figures 1 and 2). Table 1 contains the list of the differentially expressed genes with fold-change (FC) minimum of 2 for the Cu excess condition, represented as $\log_2(FC) \geq |1|$. *OsCOPT1* and metallothionein *OsMT1c*, which are respectively down- and up-regulated under Cu excess, validated our experimental settings (Figure 2). Interestingly, the expression of several genes involved in Fe homeostasis appeared to be significantly altered. Ferritin (*OsFER2*) (LOC_Os12g01530) and ferredoxin (*OsFd1*) (LOC_Os08g01380) were down-regulated, whereas nicotianamine synthase (*OsNAS2*)

(LOC_Os03g19420) and the *OsIRO2* (LOC_Os01g72370) transcription factor were induced under Cu excess (Table 1).

To validate the transcriptomic profile and further assess Cu responsiveness, quantitative RT-PCR analyses were conducted in the samples from the seedlings grown within a range of Cu concentrations (0-75 μM $CuSO_4$). The transcript levels of *OsFER2* and *OsFd1* lowered as the Cu concentration increased in the growth medium (Figure 2). On the other hand, the expression levels of *OsIRO2* and its target *OsNAS2* were up-regulated as the Cu concentration increased (Figure 2). Other OsIRO2-targets, such as *OsNAS1* and *OsNAAT1* (Ogo et al. 2007), as well as metallothionein *OsMT1f* were also induced under Cu excess (Table 1). All of them were confirmed by quantitative RT-PCR (Figure S2). Since the expression of *OsCOPT5* and *OsCOPT7* is induced by Cu deficiency (Yuan et al. 2010), they were also included as controls in the analysis. *OsCOPT7* was indeed up-regulated under the standard control condition that represents a slight Cu deficiency, as previously stated (Figures 1a and 2a), whereas *OsCOPT5* was not regulated under our experimental conditions (Figure S2). Other Fe-related genes such as those encoding Fe superoxide dismutase, *OsFSD1.1* and *OsFSD1.2,* and the Fe-sulfur domain-contain protein 1 *OsCDGSH* (displaying a Log_2(FC) value of -0.615) were down-regulated under Cu excess (Figure S3). Taken together, both global expression analysis and quantitative RT-PCR expression patterns indicate that rice Cu status influences Fe homeostasis by altering the expression of several Fe-related genes.

Ectopic expression of AtCOPT1 impacts iron homeostasis

Our global gene expression studies in rice seedling shoots suggested that Cu had an impact on Fe homeostasis (Table 1). To further investigate the cross-talk between Cu and Fe we generated two independent transgenic *O. sativa* lines that ectopically overexpressed the *Arabidopsis AtCOPT1* transport protein fused to the carboxy-terminal end to the Human Influenza Hemaglutinin epitope (HA) under the control of the cauliflower mosaic virus 35S (*CaMV35S*) promoter and the nopaline synthase (*NOS*) terminator. These *CaMV35S::AtCOPT1-HA::NOS* transgenic plants were named *AtCOPT1^{OE}-1* (*C1^{OE}-1*) and *AtCOPT1^{OE}-2* (*C1^{OE}-2*). To verify that the obtained transgenic lines expressed the *CaMV35S::AtCOPT1-HA::NOS* construct, both kanamycin-resistant plants were analyzed by different approaches. First, the *cDNA* obtained from 8 day-old WT, *C1^{OE}-1* and *C1^{OE}-2* the 8 day-old seedlings was analyzed by semiquantitative RT-PCR (Figure 3a). The *AtCOPT1* gene was detected only in the transgenic lines. Addition of the HA epitope allowed to detect AtCOPT1 protein by Western blotting (Figure 3b). Although a similar amount of total protein was processed in the three samples (lower panel in Figure 3b), the HA epitope was detected only in the *C1^{OE}* seedlings (upper panel in Figure 3b). These results corroborate that the two transgenic lines (*C1^{OE}-1* and *C1^{OE}-2*) express the *AtCOPT1* gene, which is translated into protein.

To characterize the consequences of *AtCOPT1* overexpression in rice, *C1^{OE}-1* and *C1^{OE}-2* seedlings were grown for 8 days in media with increasing Cu concentrations, and then shoot and root lengths were measured (Figure 4). In both WT and transgenic plants, shoot and root lengths decreased when 50 μM or higher Cu concentrations were added to the medium (Figure 4). Importantly, shoot and root

shortening was more pronounced in the transgenic lines. Specifically, *C1^{OE}-1* transgenic line displayed a significant decrease in shoot length as compared to WT seedlings, whereas the *C1^{OE}-2* did not display a significant difference probably due to its higher variability (Figure 4a). Regarding root length, 27% and 19% root growth reductions took place in the WT seedlings at 50 and 75 μM Cu SO_4, whereas root growth inhibition was significantly more prominent (29-52%) in both *C1^{OE}-1* and *C1^{OE}-2* lines (Figure 4b). These results indicate that *C1^{OE}* rice plants are sensitive to Cu.

To check whether the transgenic plants altered Cu and Fe accumulation, the endogenous levels of both metals were determined in roots and shoots by ICP-MS (Figure 5). At the Cu conditions assayed (0 and 75 μM added $CuSO_4$), no significant differences in shoot and root endogenous Cu levels were observed for the transgenic plants as compared to WT. With regard to Fe content, under standard control conditions (no added $CuSO_4$), the *C1^{OE}-1* and *C1^{OE}-2* roots accumulated 60-36% less Fe than the WT lines respectively (Figure 5b). These data indicate that the expression of *AtCOPT1* in rice significantly decreases root Fe accumulation.

The expression of the Cu and Fe homeostasis genes was analyzed by quantitative RT-PCR in the *C1^{OE}* transgenic plants. We selected *OsCOPT1* and *OsMT1c* as representative genes that were down- and up-regulated respectively by Cu excess (Figure 2). The endogenous *OsCOPT1* expression was lower in the two transgenic *C1^{OE}* lines at 0 μM $CuSO_4$ (Figure 6). This result suggests that, despite no global changes in plant Cu levels were observed by ICP-MS (Figure 5), the transgenic plants might sense increased nucleo-cytosolic Cu concentration. Under 75 μM $CuSO_4$, *OsMT1c* expression was higher in the two transgenic *C1^{OE}* lines than in WT seedlings (Figure 6), which also

indicates that *C1*^{OE} plants are sensing higher Cu levels. Altogether, these data indicate that the *C1*^{OE} lines display gene expression changes compatible with the perception of increased intracellular Cu levels and that the expression of specific marker genes could be more sensitive than total content of metals to assess nucleo-cytosolic Cu status.

Then we analyzed the expression of Fe-related genes. Whereas *OsFER2* expression remained mainly unchanged, *OsHRZ1, OsHRZ2, OsIRO2* and *OsFd1* expression was higher in the transgenic lines at least in 75 μM $CuSO_4$ (Figure 6). Given the postulated negative role of OsHRZ1 and OsHRZ2 in Fe acquisition (Kobayashi et al. 2013), these results point to altered Fe homeostasis when Cu uptake is increased in *C1*^{OE} lines. However, the expression of the putative Fe sensors *OsHRZ1* and *OsHRZ2* in WT plants was similar under different levels of Cu supply, with a decrease for *OsHRZ2* at 75 μM $CuSO_4$ (Figure S3).

In *Arabidopsis*, substitution of Cu-Zn superoxide dismutase (SOD) for its Fe counterpart is a specific feature of the Cu deficiency response (Abdel-Ghany et al. 2005; Waters et al. 2012). Given that SOD substitution would implicate an increased Fe demand under Cu deficiency, we checked whether it also took place in *Oryza sativa* (Figure S4). The expression of the different genes that encoded Cu-dependent SODs (*OsCSD1.1*, *OsCSD1.2* and *OsCSD2*) remained higher under control than under Cu excess conditions, instead of being repressed by low Cu as described for *Arabidopsis* homologs (Abdel-Ghany and Pilon 2008; Waters et al. 2012). The expression of Fe-dependent SODs (*OsFSD1.1* and *OsFSD1.2*) was also higher in Cu excess, which is indicative of increased superoxide radical production under the slight Cu deficiency shown by control conditions. However, no significant differences in the expression of

SOD genes were detected between the WT and *C1*^{OE} transgenic lines (Figure S4), which suggests that SOD substitution is not implicated in the observed phenotypes.

Phenotype of transgenic AtCOPT1 overexpressing lines with different copper and iron concentrations

To further investigate the potential interaction between Cu and Fe, we analyzed several parameters of the WT and *C1*^{OE} seedlings grown in the presence of different Cu and Fe concentrations (Figure 7). The WT and both *C1*^{OE} lines displayed a similar root length when grown in plates under the control medium (+Cu +Fe). However, the *C1*^{OE} transgenic lines were more sensitive to single Cu (-Cu +Fe; 35%-42% root length reduction), and especially to Fe (+Cu -Fe; 75%-69% reduction) and the double (-Cu -Fe; 71%-76% reduction) deficiencies (Figure 7). Hydroponic cultures of the WT and *C1*^{OE}*-1* lines were also performed under both the control (+Cu +Fe) and deficiency (-Cu -Fe) conditions. The adult *C1*^{OE}*-1* plants also showed differences with the controls, as indicated by the 30% reduction of chlorophyll levels when grown on hydroponic cultures under both metal sufficiency and deficiency (Figure S5).

In order to check how the WT and *C1*^{OE} rice lines performed under regular greenhouse conditions, different agronomic parameters were analyzed (Figure 8). Plant heights remained mostly unaltered, except for a slight decrease (about 15 %) in the *C1*^{OE}*-2* line (Figures 8a and 8b). Metal concentrations were determined both in young and old leaves from 4- and 5-months old plants. Whereas metals remained mostly unchanged in old leaves from 5 month-old plants, Cu and Fe concentrations increased in young leaves from *C1*^{OE} rice lines (Figure S6). Chlorophyll concentration

and panicle production per plant were not affected in the $C1^{OE}$ lines under these growing conditions (Figure 8b and 8c). However, the number of grains per panicle was slightly reduced in the $C1^{OE}$ lines (Figure 8c). The localization of Fe detected by the Perl´s staining method (Stacey et al. 2007) indicated that Fe was present in both the WT and $C1^{OE}$ lines (Figure S7). However, Cu and Fe concentration in the unpolished rice grain from both $C1^{OE}$ lines was higher than in the controls (Figure 9a). Whereas Cu concentration slightly decreased in the polished grains from the $C1^{OE}$ lines compared to the controls, Fe concentration was still higher than in the WT (Figure 9b). Altogether, ectopic expression of *AtCOPT1* in rice leads to altered Fe homeostasis with increased Fe concentration in sink organs, such as young leaves and unpolished rice grains.

Discussion

In this work, we evaluated the physiological and molecular effects caused by Cu in *O. sativa* plants when adding Cu to the media and also when plants overexpressed the high-affinity Cu transport protein COPT1 from *A. thaliana*. Rather than metal quantification, the expression of Cu homeostasis molecular markers seems a more reliable indicator of the symplastic metal status. Total metal determinations in plant cells are unable to discriminate the metal partitioning between intracellular and apoplastic compartments since metals are tightly bound to the cell walls (Ye et al. 2015). In *A. thaliana*, the expression of plasma membrane *COPT* transport genes (*AtCOPT1*, *AtCOPT2* and *AtCOPT6*) has been shown to serve as markers of Cu deficiency conditions (Sancenón et al. 2003; Andrés-Colás et al. 2010; Garcia-Molina et

al. 2013). The fact that the *OsCOPT1* expression was finely regulated according to the Cu concentration in the medium suggests that this transporter is also an excellent marker of the endogenous cellular Cu status in shoots from rice seedlings (Figure 2). Thus, when considering the *OsCOPT1* expression pattern, three different Cu level conditions were established in the media in *O. sativa*. Cu deficiency was attained in the media with no supplemented Cu (0 μM $CuSO_4$), where the *OsCOPT1* transport protein was markedly induced. Slight Cu deficiency conditions are also corroborated by increased expression of *OsCOPT7*, *OsATX1, OsFSD1.1 and OsFSD1.2* (Figures S2 and S3). Cu sufficiency conditions corresponded to the presence of 1 μM and 10 μM $CuSO_4$ in the media, where *OsCOPT1* displayed a basal expression. Cu excess in rice was observed at 50 μM $CuSO_4$ and at higher Cu concentrations (75 μM $CuSO_4$), when the *OsCOPT1* expression was barely detected (Figure 2). For Cu excess, the data from rice differed from those obtained in *Arabidopsis* since 10 μM $CuSO_4$ resulted in metal excess concentration in *Arabidopsis* (Andrés-Colás et al. 2013).

To conduct a global gene expression study 75 μM $CuSO_4$ was selected as Cu excess and compared to the standard control condition (0 μM $CuSO_4$). *OsMT1c* induction confirmed that the presence of 50 μM and 75 μM $CuSO_4$ in the media represented metal excess (Figure 2). Another *MT* gene *OsMT1f* was also induced under Cu excess (Table 1 and Figure S2), which is indicative of them being good candidates for molecular markers of Cu excess in rice. The induction of type 1 metallothioneins under Cu excess is a well-known protecting process that affects ROS scavenging or signaling (Hassinen et al. 2011). The expression of genes related to NA-metal

complexes, such as *OsNAS1*, *OsNAS2* and *OsNAAT1* were also increased (Figures 2 and S2), and could be used as molecular markers of Cu excess in rice.

To examine the effect of altered Cu incorporation, we overexpressed *AtCOPT1* in the *O. sativa* plants. AtCOPT1 shares 51% sequence identity and 66% sequence similarity with OsCOPT1 (Yuan et al. 2010). Moreover, AtCOPT1 is able to complement the phenotype of *S. cerevisiae* strains deficient in Cu transport (Puig and Thiele 2002; Sancenón et al. 2003). We confirmed that the $C1^{OE}$ rice lines generated expressed the heterologous gene and produced the encoded protein (Figure 3). At the phenotypic level, and under Cu excess conditions, the shortening of root length was more marked in the $C1^{OE}$ plants than in the WT (Figure 4). These results are consistent with those described in *Arabidopsis* (Andrés-Colás et al. 2010), and agree with previous studies in which Cu excess was found to cause a reduction in the weight of rice plants (Mostofa et al. 2014). This could be due to the incorporation of Cu into plants as Cu(I), which is harmful as it produces ROS (Rodrigo-Moreno et al. 2013). The reduced expression of the endogenous *OsCOPT1* gene in the transgenic lines under standard control conditions indicated that the $C1^{OE}$ lines perceived more endogenous Cu levels as a result of AtCOPT1 activity (Figure 6). Likewise, the highest expression of the metallothionein *OsMT1c* under Cu excess (Figure 6) further indicated increased Cu perception in the $C1^{OE}$ lines.

There is evidence for the relationship between Cu and Fe in other organisms, such as yeast or algae, where Cu is necessary for Fe incorporation and distribution (Puig et al. 2007; Gulec and Collins 2014). In *Arabidopsis*, Cu and Fe deficiencies induce the expression of high-affinity Cu transport protein *COPT2,* and that *copt2* mutants are

more tolerant than WT plants to double Cu and Fe deficiencies (Colangelo and Guerinot 2004; Perea-García et al. 2013). In agreement with these data, *AtCOPT1* overexpression in rice produced increased sensitivity to double Cu and Fe deficiencies (Figures 7 and S5). Severe Cu deficiency leads to increased auxin synthesis in rice (Figure 1c), as described for Fe deficiency in *Arabidopsis*, which results in the enhanced expression of Fe-deficiency genes (Chen et al. 2010). Although the role of IAA in the cross-talk between Cu and Fe homeostasis merits further characterization (Peñarrubia et al. 2015), our results envisage that plants subjected to multiple nutritional deficiencies also face an auxin dilemma.

The putative Fe and oxygen/redox state sensors *OsHRZ1* and *OsHRZ2* have been shown to act as a negative regulators of Fe homeostasis (Kobayashi et al. 2013). *OsHRZ1* and *OsHRZ2* expression could be affected by the effects of Cu(I)-uptake since increased in $C1^{OE}$ plants (Figure 6), but not under Cu excess (Figure S3).

Cu-Fe crosstalk under Cu excess might be at least partially explained by the increased expression of the transcriptional regulator *OsIRO2,* which could justify the expression of the Fe strategy II uptake targets related to DMA biosynthesis, such as *OsNAS1*, *OsNAS2* and *OsNAAT1* (Table 1 and Figures 2 and S2) (Ogo et al. 2007). *OsIRO2* expression is subjected to the control of postulated Fe sensor OsIDEF1. By using the recombinant OsIDEF1 protein in *in vitro* experiments, Kobayashi and coauthors (2012) demonstrated that OsIDEF1 binds Fe(II) and other divalent metals, including Cu(II), through its histidine-asparagine repeat and proline-rich regions. Based on its ability to bind metals in proportion to their cellular abundance, it is tempting to speculate that Cu(II) could exert the described influence by competing with Fe(II) in

OsIDEF1 metal-binding domains. In agreement with this, OsIDEF1 has been proposed to sense the nutritional metal balance by detecting the ratio of Fe to other metals rather than absolute Fe concentration (Kobayashi et al. 2012). Thus, Cu excess could affect at least some of the Fe deficiency responses, such as those leading to the increased expression of *OsIRO2* and its downstream targets.

Cu and Fe concentrations in the different plant organs are probably the result of multiple processes in which both metals face diverse and complex interactions in their way from source toward sink organs including seeds. NA functions in a phloem pathway for Fe translocation to sink organs (Tsukamoto et al. 2009). Since Cu(II)-NA complexes are very stable (von Wirén et al. 1999), increased expression of *OsNAS1*, *OsNAS2* and *OsNAAT1* under Cu excess (Figures 2 and S2) could reflect not only the increased Cu content, but could also affect Fe mobilization and accumulation in sink organs. As observed here, Fe concentration increased in young leaves as the plants got older (Figure S6). Based on the lower Fe concentration in *COPT*-overexpressing roots under Cu scarce media (Fig. 5b), it is tempting to speculate that a putative Fe deficiency signaling could result in increased Fe mobilization to the sink organs. Interestingly, the Fe concentration of polished and unpolished rice grains from $C1^{OE}$ plants increased 60% and 30% respectively (Figure 9). Otherwise, the $C1^{OE}$ plants were similar to the WT in agronomic performance terms when grown under regular greenhouse conditions (Figures 8). However, the approximate 8 μg of Fe/g DW obtained by this approach (Figure 9) is lower than the concentrations obtained by other strategies which range from 10-19 μg of Fe/g DW (Johnson et al. 2011; Oliva et al. 2014; Boonyaves et al. 2016; Trijatmiko et al. 2016). Taken together, these results

indicate that both Cu deficiency and Cu excess may interfere with Fe sensing and mobilization in rice. The understanding of these interactions could be useful to design biotechnological approaches to improve the nutritional Fe concentration of edible crop parts.

References

Abdel-Ghany SE, Burkhead JL, Gogolin KA, Andrés-Colás N, Bodecker JR, Puig S, Peñarrubia L, Pilon M (2005) AtCCS is a functional homolog of the yeast copper chaperone Ccs1/Lys7. FEBS Lett 579:2307–2312. doi: http://dx.doi.org/10.1016/j.febslet.2005.03.025

Abdel-Ghany SE, Pilon M (2008) MicroRNA-mediated systemic down-regulation of copper protein expression in response to low copper availability in *Arabidopsis*. J Biol Chem 283:15932–15945. doi: 10.1074/jbc.M801406200

Andrés-Colás N, Perea-García A, Mayo de Andrés S, Garcia-Molina A, Dorcey E, Rodríguez-Navarro S, Pérez-Amador MA, Puig S, Peñarrubia L, Mayo de Andres S, García-Molina A, Dorcey E, Rodriguez-Navarro S, Perez-Amador MA, Puig S, Peñarrubia L (2013) Comparison of global responses to mild deficiency and excess copper levels in *Arabidopsis* seedlings. Metallomics 5:1234–1246. doi: 10.1039/c3mt00025g

Andrés-Colás N, Perea-García A, Puig S, Peñarrubia L (2010) Deregulated copper transport affects *Arabidopsis* development especially in the absence of environmental cycles. Plant Physiol 153:170–184. doi: 10.1104/pp.110.153676

Andrés F, Galbraith DW, Talón M, Domingo C (2009) Analysis of PHOTOPERIOD SENSITIVITY5 sheds light on the role of phytochromes in photoperiodic flowering in rice. Plant Physiol 151:681–690. doi: 10.1104/pp.109.139097

Benjamini Y, Hochberg Y (1995) Controlling the false discovery rate: a practical and powerful approach to multiple testing. J R Stat Soc Ser B 57:289–300. doi: 10.2307/2346101

Bernal M, Casero D, Singh V, Wilson GT, Grande A, Yang H, Dodani SC, Pellegrini M, Huijser P, Connolly EL, Merchant SS, Krämer U (2012) Transcriptome sequencing identifies *SPL7*-regulated copper acquisition genes *FRO4*/*FRO5* and the copper dependence of iron homeostasis in *Arabidopsis*. Plant Cell 24:738–761. doi: 10.1105/tpc.111.090431

Bhullar NK, Gruissem W (2013) Nutritional enhancement of rice for human health: The contribution of biotechnology. Biotechnol Adv 31:50–57. doi: 10.1016/j.biotechadv.2012.02.001

Boonyaves K, Gruissem W, Bhullar NK (2016) NOD promoter-controlled AtIRT1 expression functions synergistically with *NAS* and *FERRITIN* genes to increase iron in rice grains. Plant Mol Biol 90:207–215. doi: 10.1007/s11103-015-0404-0

Briat JF (1996) Roles of ferritin in plants. J Plant Nutr 19:1331–1342. doi: 10.1080/01904169609365202

Chen WW, Yang JL, Qin C, Jin CW, Mo JH, Ye T, Zheng SJ (2010) Nitric oxide acts downstream of auxin to trigger root ferric-chelate reductase activity in response to iron deficiency in *Arabidopsis*. Plant Physiol 154:810–819. doi: 10.1104/pp.110.161109

Colangelo EP, Guerinot ML (2004) The essential basic helix-loop-helix protein FIT1 is required for the iron deficiency response. Plant Cell 16:3400–3412. doi: 10.1105/tpc.104.024315

Crichton RR, Pierre JL (2001) Old iron, young copper : from mars to venus. Biometals 14:99–112. doi: 10.1023/A:1016710810701

Di Rienzo JA, Casanoves F, Balzarini MG, Gonzalez L, Tablada M, Robledo CW (2011) InfoStat.

Garcia-Molina A, Andrés-Colás N, Perea-García A, Del Valle-Tascõn S, Peñarrubia L, Puig S (2011) The intracellular *Arabidopsis* COPT5 transport protein is required for photosynthetic electron transport under severe copper deficiency. Plant J 65:848–860. doi: 10.1111/j.1365-313X.2010.04472.x

Garcia-Molina A, Andrés-Colás N, Perea-García A, Neumann U, Dodani SC, Huijser P, Peñarrubia L, Puig S (2013) The *Arabidopsis* COPT6 transport protein functions in copper distribution under copper-deficient conditions. Plant Cell Physiol 54:1378–1390. doi: 10.1093/pcp/pct088

Goto F, Yoshihara T, Shigemoto N, Toki S, Takaiwa F (1999) Iron fortification of rice seed by the soybean ferritin gene. Nat Biotechnol 17:282–286. doi: 10.1038/7029

Gulec S, Collins JF (2014) Molecular mediators governing iron-copper interactions. Annu Rev Nutr 34:95–116. doi: 10.1146/annurev-nutr-071812-161215

Hassinen VH, Tervahauta AI, Schat H, Kärenlampi SO (2011) Plant metallothioneins – metal chelators with ROS scavenging activity? Plant Biol 13:225–232. doi: 10.1111/j.1438-8677.2010.00398.x

Hermans C, Bourgis F, Faucher M, Strasser RJ, Delrot S, Verbruggen N (2005) Magnesium deficiency in sugar beets alters sugar partitioning and phloem loading in young mature leaves. Planta 220:541–549. doi: 10.1007/s00425-004-1376-5

Hiei Y, Ohta S, Komari T, Kumashiro T (1994) Efficient transformation of rice (*Oryza sativa L.*) mediated by *Agrobacterium* and sequence analysis of the boundaries of the T-DNA. Plant J 6:271–282. doi: 10.1046/j.1365-313X.1994.6020271.x

Ishimaru Y, Masuda H, Bashir K, Inoue H, Tsukamoto T, Takahashi M, Nakanishi H, Aoki N, Hirose T, Ohsugi R, Nishizawa NK (2010) Rice metal-nicotianamine transporter, OsYSL2, is required for the long-distance transport of iron and manganese. Plant J 62:379–390. doi: 10.1111/j.1365-313X.2010.04158.x

Ishimaru Y, Suzuki M, Tsukamoto T, Suzuki K, Nakazono M, Kobayashi T, Wada Y, Watanabe S, Matsuhashi S, Takahashi M, Nakanishi H, Mori S, Nishizawa NK (2006) Rice plants take up iron as an Fe^{3+}-phytosiderophore and as Fe^{2+}. Plant J 45:335–346. doi: 10.1111/j.1365-313X.2005.02624.x

Johnson AAT, Kyriacou B, Callahan DL, Carruthers L, Stangoulis J, Lombi E, Tester M (2011) Constitutive overexpression of the *OsNAS* gene family reveals single-gene strategies for effective iron- and zinc-biofortification of rice endosperm. PLoS One 6:e24476. doi: 10.1371/journal.pone.0024476

Kobayashi T, Itai RN, Aung MS, Senoura T, Nakanishi H, Nishizawa NK (2012) The rice transcription factor IDEF1 directly binds to iron and other divalent metals for sensing cellular iron status. Plant J 69:81–91. doi: 10.1111/j.1365-313X.2011.04772.x

Kobayashi T, Nagasaka S, Senoura T, Itai RN, Nakanishi H, Nishizawa NK (2013) Iron-binding Haemerythrin RING ubiquitin ligases regulate plant iron responses and accumulation. Nat Commun 4:2792. doi: 10.1038/ncomms3792

Kobayashi T, Nishizawa NK (2012) Iron uptake, translocation, and regulation in higher plants. Annu Rev Plant Biol 63:131–152. doi: 10.1146/annurev-arplant-042811-105522

Kobayashi T, Nishizawa NK (2014) Iron sensors and signals in response to iron deficiency. Plant Sci 224:36–43. doi: http://dx.doi.org/10.1016/j.plantsci.2014.04.002

Koike S, Inoue H, Mizuno D, Takahashi M, Nakanishi H, Mori S, Nishizawa NK (2004) OsYSL2 is a rice metal-nicotianamine transporter that is regulated by iron and expressed in the phloem. Plant J 39:415–424. doi: 10.1111/j.1365-313X.2004.02146.x

Lee SSJ, Jeon US, Lee SSJ, Kim Y-K, Persson DP, Husted S, Schjørring JK, Kakei Y, Masuda H, Nishizawa NK, An G (2009) Iron fortification of rice seeds through activation of the nicotianamine synthase gene. Proc Natl Acad Sci 106:22014–22019. doi: 10.1073/pnas.0910950106

Leszczyszyn OI, Imam HT, Blindauer C a (2013) Diversity and distribution of plant metallothioneins: a review of structure, properties and functions. Metallomics 5:1146–1169. doi: 10.1039/c3mt00072a

Marschner P (2012) Marschner's Mineral Nutrition of Higher Plants, Third Edition.

Mostofa MG, Seraj Z, Fujita M (2014) Exogenous sodium nitroprusside and glutathione alleviate copper toxicity by reducing copper uptake and oxidative damage in rice (*Oryza sativa L.*) seedlings. Protoplasma 251:1373–1386. doi: 10.1007/s00709-014-0639-7

Murashige T, Skoog F (1962) A revised medium for rapid growth and bio assays with tobacco tissue cultures. Physiol Plant 15:493–497.

Ogo Y, Itai RN, Kobayashi T, Aung MS, Nakanishi H, Nishizawa NK (2011) OsIRO2 is responsible for iron utilization in rice and improves growth and yield in calcareous soil. Plant Mol Biol Volume 75:593–605. doi: 10.1007/s11103-011-9752-6

Ogo Y, Itai RN, Nakanishi H, Inoue H, Kobayashi T, Suzuki M, Takahashi M, Mori S, Nishizawa NK (2006) Isolation and characterization of IRO2, a novel iron-regulated bHLH transcription factor in graminaceous plants. J Exp Bot 57:2867–2878. doi: 10.1093/jxb/erl054

Ogo Y, Nakanishi Itai R, Nakanishi H, Kobayashi T, Takahashi M, Mori S, Nishizawa NK (2007) The rice bHLH protein OsIRO2 is an essential regulator of the genes involved in Fe uptake under Fe-deficient conditions. Plant J 51:366–377. doi: 10.1111/j.1365-313X.2007.03149.x

Oliva N, Chadha-Mohanty P, Poletti S, Abrigo E, Atienza G, Torrizo L, Garcia R, Dueñas C, Poncio MA, Balindong J, Manzanilla M, Montecillo F, Zaidem M, Barry G, Hervé P, Shou H, Slamet-Loedin IH (2014) Large-scale production and evaluation of marker-free indica rice IR64 expressing phytoferritin genes. Mol Breed 33:23–37. doi: 10.1007/s11032-013-9931-z

Peñarrubia L, Romero P, Carrió-Seguí A, Andrés-Bordería A, Moreno J, Sanz A (2015) Temporal aspects of copper homeostasis and its crosstalk with hormones. Front Plant Sci 6:1–18. doi: 10.3389/fpls.2015.00255

Perea-García A, Garcia-Molina A, Andrés-Colás N, Vera-Sirera F, Pérez-Amador MA, Puig S, Peñarrubia L (2013) *Arabidopsis* copper transport protein COPT2 participates in the

crosstalk between iron deficiency responses and low phosphate signaling. Plant Physiol 162:180–194. doi: 10.1104/pp.112.212407

Pfaffl MW (2001) A new mathematical model for relative quantification in real-time RT–PCR. Nucleic Acids Res 29:e45. doi: 10.1093/nar/29.9.e45

Puig S (2014) Function and regulation of the plant COPT family of high-affinity copper transport proteins. Adv Bot 2014:1–9. doi: 10.1155/2014/476917

Puig S, Andrés-Colás N, García-Molina A, Peñarrubia L (2007) Copper and iron homeostasis in *Arabidopsis*: Responses to metal deficiencies, interactions and biotechnological applications. Plant, Cell Environ 30:271–290. doi: 10.1111/j.1365-3040.2007.01642.x

Puig S, Peñarrubia L (2009) Placing metal micronutrients in context: transport and distribution in plants. Curr Opin Plant Biol 12:299–306. doi: 10.1016/j.pbi.2009.04.008

Puig S, Thiele DJ (2002) Molecular mechanisms of copper uptake and distribution. Curr Opin Chem Biol 6:171–180. doi: http://dx.doi.org/10.1016/S1367-5931(02)00298-3

Ravet K, Pilon M (2013) Copper and iron homeostasis in plants: the challenges of oxidative stress. Antioxid Redox Signal 19:919–932. doi: 10.1089/ars.2012.5084

Rodrigo-Moreno A, Andrés-Colás N, Poschenrieder C, Gunsé B, Peñarrubia L, Shabala S (2013) Calcium- and potassium-permeable plasma membrane transporters are activated by copper in *Arabidopsis* root tips: linking copper transport with cytosolic hydroxyl radical production. Plant Cell Environ 36:844–855. doi: 10.1111/pce.12020

Sancenón V, Puig S, Mira H, Thiele DJ, Peñarrubia L (2003) Identification of a copper transporter family in *Arabidopsis thaliana*. Plant Mol Biol 51:577–587. doi: 10.1023/a:1022345507112

Smyth GK (2005) Limma: Linear Models for Microarray Data. New York.

Sperotto RA, Ricachenevsky FK, Waldow V de A, Fett JP (2012) Iron biofortification in rice: It's a long way to the top. Plant Sci 190:24–39. doi: 10.1016/j.plantsci.2012.03.004

Stacey MG, Patel A, McClain WE, Mathieu M, Remley M, Rogers EE, Gassmann W, Blevins DG, Stacey G (2007) The *Arabidopsis* AtOPT3 protein functions in metal homeostasis and movement of iron to developing seeds. PLANT Physiol 146:589–601. doi: 10.1104/pp.107.108183

Stevens GA, Finucane MM, De-Regil LM, Paciorek CJ, Flaxman SR, Branca F, Peña-Rosas JP, Bhutta ZA, Ezzati M (2013) Global, regional, and national trends in haemoglobin concentration and prevalence of total and severe anaemia in children and pregnant and non-pregnant women for 1995–2011: a systematic analysis of population-representative. Lancet Glob Heal 1:e16–e25. doi: 10.1016/S2214-109X(13)70001-9

Trijatmiko KR, Dueñas C, Tsakirpaloglou N, Torrizo L, Arines FM, Adeva C, Balindong J, Oliva N, Sapasap M V, Borrero J, Rey J, Francisco P, Nelson A, Nakanishi H, Lombi E, Tako E, Glahn RP, Stangoulis J, Chadha-Mohanty P, Johnson AAT, Tohme J, Barry G, Slamet-Loedin IH (2016) Biofortified indica rice attains iron and zinc nutrition dietary targets in the field. Sci Rep 6:19792. doi: 10.1038/srep19792

Tsukamoto T, Nakanishi H, Uchida H, Watanabe S, Matsuhashi S, Mori S, Nishizawa NK (2009) ^{52}Fe translocation in barley as monitored by a positron-emitting tracer imaging system (PETIS): Evidence for the direct translocation of Fe from roots to young leaves via phloem. Plant Cell Physiol 50:48–57. doi: 10.1093/pcp/pcn192

von Wirén N, Klair S, Bansal S, Briat J-F, Khodr H, Shioiri T, Leigh RA, Hider RC (1999) Nicotianamine chelates both FeIII and FeII. Implications for metal transport in plants. Plant Physiol 119:1107–1114. doi: 10.1104/pp.119.3.1107

Waters BM, Armbrust LC (2013) Optimal copper supply is required for normal plant iron deficiency responses. Plant Signal Behav 8:e26611. doi: 10.4161/psb.26611

Waters BM, McInturf SA, Stein RJ (2012) Rosette iron deficiency transcript and microRNA profiling reveals links between copper and iron homeostasis in *Arabidopsis thaliana*. J Exp Bot 63:5903–5918. doi: 10.1093/jxb/ers239

White PJ, Broadley MR (2009) Biofortification of crops with seven mineral elements often lacking in human diets – iron, zinc, copper, calcium, magnesium, selenium and iodine. New Phytol 182:49–84. doi: 10.1111/j.1469-8137.2008.02738.x

Yamasaki H, Hayashi M, Fukazawa M, Kobayashi Y, Shikanai T (2009) SQUAMOSA Promoter binding Protein–like7 is a central regulator for copper homeostasis in *Arabidopsis*. Plant Cell 21:347–361. doi: 10.1105/tpc.108.060137

Ye Y, Yuan J, Chang X, Yang M, Zhang L, Lu K, Lian X (2015) The phosphate transporter gene *OsPht1;4* is involved in phosphate homeostasis in rice. PLoS One 10:e0126186. doi: 10.1371/journal.pone.0126186

Yruela I (2013) Transition metals in plant photosynthesis. Metallomics 5:1090–1109. doi: 10.1039/c3mt00086a

Yuan M, Chu Z, Li X, Xu C, Wang S (2010) The bacterial pathogen *Xanthomonas oryzae* overcomes rice defenses by regulating host copper redistribution. Plant Cell 22:3164–3176. doi: 10.1105/tpc.110.078022

Yuan M, Li X, Xiao J, Wang S (2011) Molecular and functional analyses of COPT/Ctr-type copper transporter-like gene family in rice. BMC Plant Biol 11:69–80. doi: 10.1186/1471-2229-11-69

Table 1. Differentially expressed genes under Cu excess. Comparison of gene expression in microarray experiments from WT *O. sativa* 8-day old seedlings germinated and grown under Cu excess (75 µM $CuSO_4$) vs control (0 µM $CuSO_4$) conditions (p-value < 0.05). Differentially expressed genes with a minimum 2-fold difference ($log_2FC \geq | 1 |$) are shown.

Gene Name	Gene ID	Annotation	log_2FC	p-value
		Repressed genes under Cu excess		
	LOC_Os01g10400	expressed protein	-1.743	1.08^{e-05}
OsCOPT1	**LOC_Os01g56420**	**ctr copper transporter family protein, putative, expressed**	**-1.590**	**8.02^{e-07}**
	LOC_Os06g39730	#N/A	-1.332	1.96^{e-03}
OsATX1	**LOC_Os02g32814**	**heavy metal-associated domain containing protein, expressed**	**-1.242**	**5.98^{e-04}**
OsAP2_ERF	LOC_Os09g11460	AP2 domain containing protein, expressed	-1.236	7.01^{e-05}
OsFER2	**LOC_Os12g01530**	**ferritin-1, chloroplast precursor, putative, expressed**	**-1.188**	**1.97^{e-05}**
OsFd1	**LOC_Os08g01380**	**2Fe-2S iron-sulfur cluster binding domain containing protein, expressed**	**-1.092**	**3.33^{e-06}**
	chr05:11696945	#N/A	-1.016	2.30^{e-06}
	LOC_Os06g41610	retrotransposon protein, putative, unclassified, expressed	-1.002	1.70^{e-03}
	LOC_Os12g08790	TPR domain protein, putative, expressed	-0.999	3.21^{e-03}
		Induced genes under Cu excess		
	LOC_Os12g38064	#N/A	3.22	3.04^{e-06}
OsNAS2	**LOC_Os03g19420**	**nicotianamine synthase, putative, expressed**	**2.18**	**1.61^{e-03}**
OsMT1c	**LOC_Os12g38010**	**metallothionein, putative, expressed**	**2.13**	**9.38^{e-08}**
OsMT1f	**LOC_Os12g38051**	**metallothionein, putative, expressed**	**2.09**	**6.78^{e-04}**
OsIRO2	**LOC_Os01g72370**	**helix-loop-helix DNA-binding domain containing protein, expressed**	**1.97**	**8.37^{e-08}**
OsNAS1	**LOC_Os03g19427**	**nicotianamine synthase, putative, expressed**	**1.80**	**3.41^{e-06}**
	LOC_Os03g32490	DUF1230 domain containing protein, expressed	1.74	5.29^{e-06}
OsNAAT1	**LOC_Os02g20360**	**tyrosine aminotransferase, putative, expressed**	**1.73**	**2.06^{e-03}**
	LOC_Os01g46720	expressed protein	1.55	1.31^{e-04}
	LOC_Os08g43840	expressed protein	1.41	9.44^{e-04}
	LOC_Os12g42960	expressed protein	1.37	2.54^{e-06}
	LOC_Os01g35310	expressed protein	1.31	1.62^{e-04}
OsSKP1	LOC_Os06g02350	S-phase kinase-associated protein 1A, putative, expressed	1.31	7.80^{e-03}
	LOC_Os03g01090	peptidyl-prolyl cis-trans isomerase, cyclophilin type, putative, expressed	1.31	1.34^{e-04}
	LOC_Os05g15770	#N/A	1.23	5.06^{e-02}
	LOC_Os11g29370	haloacid dehalogenase-like hydrolase family protein, putative, expressed	1.18	1.25^{e-04}
OsLEA1	LOC_Os03g20680	late embryogenesis abundant protein 1, putative, expressed	1.16	5.57^{e-04}
	LOC_Os05g38210	mitochondrial glycoprotein, putative, expressed	1.14	8.86^{e-03}
	LOC_Os08g08170	transposon protein, putative, CACTA, En/Spm sub-class	1.11	4.49^{e-02}
	chr03:307064	#N/A	1.10	1.30^{e-03}
	LOC_Os10g14050	expressed protein	1.06	2.30^{e-04}
OsRNAsaT2	LOC_Os09g36680	ribonuclease T2 family domain containing protein, expressed	1.04	3.57^{e-04}
	LOC_Os09g17590	expressed protein	1.00	1.21^{e-03}
	LOC_Os03g38970	metal ion binding protein, putative, expressed	1.00	1.19^{e-05}

Log_2FC= Logarithm of fold change to the base 2. Genes in bold have been used along this work to validate their gene expression patterns by quantitative RT-PCR.

Figure legends

Fig. 1 Characterization of *O. sativa* plants grown in media with different Cu concentrations. (a) Endogenous Cu concentration of the 8 day-old seedling shoots from the WT plants grown on a Cu scale that ranged from control conditions (0 µM $CuSO_4$) with slight Cu deficiency to severe excess (100 µM $CuSO_4$). Cu was determined by atomic absorption spectrophotometry. (b) Root length of the WT plants grown under the same conditions indicated in (a). (c) IAA concentration of WT seedlings shoots grown under severe Cu deficiency (BCS 100 µM) or Cu sufficiency (10 µM $CuSO_4$). Values are the mean±SD of n=3 replicates. The samples with a common letter are not significantly different (p-value >0.05) Kruskal-Wallis test.

Fig. 2 Expression of genes involved in metal homeostasis at different Cu contents. (a) Relative expression of the genes induced under low Cu. Expression of *OsCOPT1*, Os*FER2* and Os*Fd1* was determined by qRT-PCR from the 8 day-old WT seedling shoots grown on a Cu scale that ranged from control conditions (0 µM $CuSO_4$) with slight Cu deficiency to metal excess (75 µM $CuSO_4$). (b) Relative expression of the genes induced under Cu excess. Expression of *OsMT1c*, *OsNAS2* and *OsIRO2* under the same conditions indicated in (a). The *Actin* gene was used as a loading control. The mRNA level is expressed in relative units (ru). The values are relative to the expression level at 0 µM $CuSO_4$ in (a) and also to the expression level at 75 µM $CuSO_4$ in (b). Values are the mean±SD of n=3 replicates. Samples with a common letter are not significantly different (p-value> 0.05).

Fig. 3 *AtCOPT1* expression in *O. sativa* transgenic plants. (a) *AtCOPT1* gene expression was determined by sqRT-PCR of the 8 day-old seedlings from the WT and $C1^{OE}$*-1* and $C1^{OE}$*-2* plants. The *18S* gene was used as a loading control. (b) A Western-blot analysis was used to detect the HA epitope of the seedlings from the WT and $C1^{OE}$*-1* and $C1^{OE}$*-2* plants grown under the same conditions indicated in (a). The anti-HA primary antibody labelled with peroxidase was used for Human Influenza Hemaglutinin epitope (HA) epitope detection. Ponceau staining was used as a loading control.

Fig. 4 Length of shoots and roots of *O. sativa* WT and $C1^{OE}$ plants. (a) The relative shoot length of the 8 day-old seedlings from the WT, $C1^{OE}$*-1* and $C1^{OE}$*-2* lines grown on a Cu scale that ranged from control conditions (0 µM $CuSO_4$) to Cu excess (75 µM $CuSO_4$). (b) The relative root length was measured under the same conditions indicated in (a). The ratio was calculated and normalized against each genotype sufficiency condition (1 µM $CuSO_4$). Values are the mean±SD of n=3 replicates. Samples with a common letter are not significantly different (p-value >0.05).

Fig. 5 Metal concentration of *O. sativa* $C1^{OE}$ plants grown in media with a different Cu status. (a) Cu concentration of the shoots and roots of the 8-day-old seedlings from the WT, $C1^{OE}$*-1* and $C1^{OE}$*-2* lines grown under control conditions (0 µM $CuSO_4$) or excess (75 µM $CuSO_4$) of Cu. (b) Fe concentration of the shoots and roots of the seedlings from WT, $C1^{OE}$*-1* and $C1^{OE}$*-2* grown under the same conditions indicated in (a). Values are the mean±SD of n=3 replicates. Samples with a common letter are not significantly different (p-value >0.05).

Fig. 6 Relative expression of *OsCOPT1*, OsCOPT7, *OsMT1c*, *OsFd1*, *OsFER2*, *OsHRZ1*, *OsHRZ2* and *OsIRO2* genes in the WT and *AtCOPT1* overexpressing rice plants**.** Relative gene expression analyzed by qRT-PCR of the WT and $C1^{OE}$ 8-day-old seedling shoots grown under control conditions (0 µM $CuSO_4$) and excess (75 µM $CuSO_4$). The *Actin* gene was used as a loading control. The mRNA level is expressed in relative units (ru). Expression values are relative to the WT seedlings grown under Cu deficiency conditions. Values are the mean±SD of n=3 replicates. Samples with a common letter are not significantly different (p-value >0.05).

Fig. 7 Characterization of the *O. sativa* $C1^{OE}$ plants grown in media with different Cu and Fe contents. (a) Representative photographs of the WT, $C1^{OE}$*-1* and $C1^{OE}$*-2* plants grown with different media: Cu and Fe sufficiency (+Cu+Fe), Cu deficiency (-Cu+Fe), Fe deficiency (+Cu-Fe), Cu and Fe deficiency (-Cu-Fe). (b) Root length of the 8 day-old seedlings of the WT, $C1^{OE}$*-1* and $C1^{O}$ *-2* plants grown under the same conditions as in (a). Represented values are the mean±SD of n=3 replicates. Samples with a common letter are not significantly different (p-value>0.05).

Fig. 8 Characterization of the *O. sativa* $C1^{OE}$ plants grown under greenhouse conditions. (a) Representative photographs of the 5 month-old from the WT, $C1^{OE}$*-1* and $C1^{OE}$*-2* plants and panicles. (b) Plant height and leaf chlorophyll content per gram of fresh weight of the rice WT and $C1^{OE}$ plants**.** (c) Panicles per plant and grain per panicle of the WT and $C1^{OE}$ plants. Represented values are the mean±SD of n=3 replicates. Samples with a common letter are not significantly different (p-value >0.05).

Fig. 9 Metal seed concentration in the *O. sativa* $C1^{OE}$ plants grown under greenhouse conditions. (a) Cu and Fe concentrations of the brown rice grain of the WT and $C1^{OE}$ plants. (b) Cu and Fe concentrations of the white rice grain of the WT and $C1^{OE}$ plants. Represented values are the mean±SD of n=3 replicates. Samples with a common letter are not significantly different (p-value>0.05).

Supplemental figures

Fig. S1 Hormone concentration in *O. sativa* plants. (a) ABA concentration of the 8 day-old seedlings of the WT plants grown under severe deficiency (BCS 100 µM) or sufficiency (10 µM $CuSO_4$) of Cu. (b) JA concentration of the 8 day-old seedlings of the WT plants grown under same conditions as in (a). Represented values are the mean±SD of n=3 replicates. Samples with a common letter are not significantly different (p-value >0.05).

Fig. S2 Gene expression in the WT plants with different Cu status. (a) Relative gene expression of *OsCOPT5*, *OsCOPT7*, *OsATX1* of the WT 8-day-old seedlings grown on control conditions (0 µM $CuSO_4$) and excess (75 µM $CuSO_4$). (b) Relative gene expression of *OsNAS1*, *NAAT1*, *OsMt1f* of the WT 8-day-old seedlings shoots grown in same conditions as in (a). Expression values are relative to the values of seedlings grown under Cu deficiency conditions. Represented values are the mean±SD of n=3 replicates. Samples with a common letter are not significantly different (p-value>0.05).

Fig. S3 Gene expression in the WT plants with different Cu status. (a) Relative gene expression of *OsFSD1.1*, *OsFSD1.2*, *OsCDGSH* of the WT 8-day-old seedlings shoots grown on a Cu scale from control conditions (0 µM $CuSO_4$) to excess (75 µM $CuSO_4$). (b) Relative gene expression of *OsHRZ1* and *OsHRZ2* of the WT 8-day-old seedlings grown in same conditions as in (a). Expression values are relative to the values of seedlings grown under Cu deficiency conditions. Represented values are the mean±SD of n=3 replicates. Samples with a common letter are not significantly different (p-value>0.05).

Fig. S4 The SOD gene expression of the WT and *AtCOPT1* overexpressing rice plants. Relative expression of genes *OsCSD1.1*, Os*CSD1.2*, Os*CSD2* (encoding Cu, Zn SODs), *OsFSD1.1* and *OsFSD1.2* (encoding Fe SODs) of the WT and $C1^{OE}$ 8-day-old seedling shoots grown under control conditions (0 µM $CuSO_4$) and excess (75 µM $CuSO_4$). Expression values are relative to the WT seedlings grown under Cu deficiency. Represented values are the mean±SD of n=3 replicates.

Fig. S5 Characterization of the WT and *AtCOPT1* overexpressing rice plants grown in hydroponic cultures. (a) Representative photographs of 1 month-old plants. The WT and $C1^{OE}$*-1* plants were grown in different hydroponic cultures under different Cu and Fe conditions: Cu and Fe sufficiency (+Cu+Fe) and double Cu and Fe deficiency (-Cu-Fe). (b) Leaf chlorophyll content. Values of chlorophyll per gram of fresh weight of the WT and $C1^{OE}$*-1* 1 month-old plants grown under the same conditions as in (a). Represented values are the mean±SD of n=3 replicates. Samples with a common letter are not significantly different (p-value >0.05).

Fig. S6 Metal concentration of the WT and *AtCOPT1* overexpressing rice plants grown in soil. (a) Cu concentration in young and old leaves of the WT and $C1^{OE}$ from 4 and 5 month-old plants grown in soil (b) Fe concentration of the WT and $C1^{OE}$ plants grown under the same conditions as in (a). Represented values are the mean±SD of n=3 replicates. Samples with a common letter are not significantly different (p-value> 0.05).

Fig. S7 Perl´s staining of the brown rice grain of the WT and $C1^{OE}$ plants. Seeds were germinated for 3 days in ½MS and photographed after Perl´s stained.

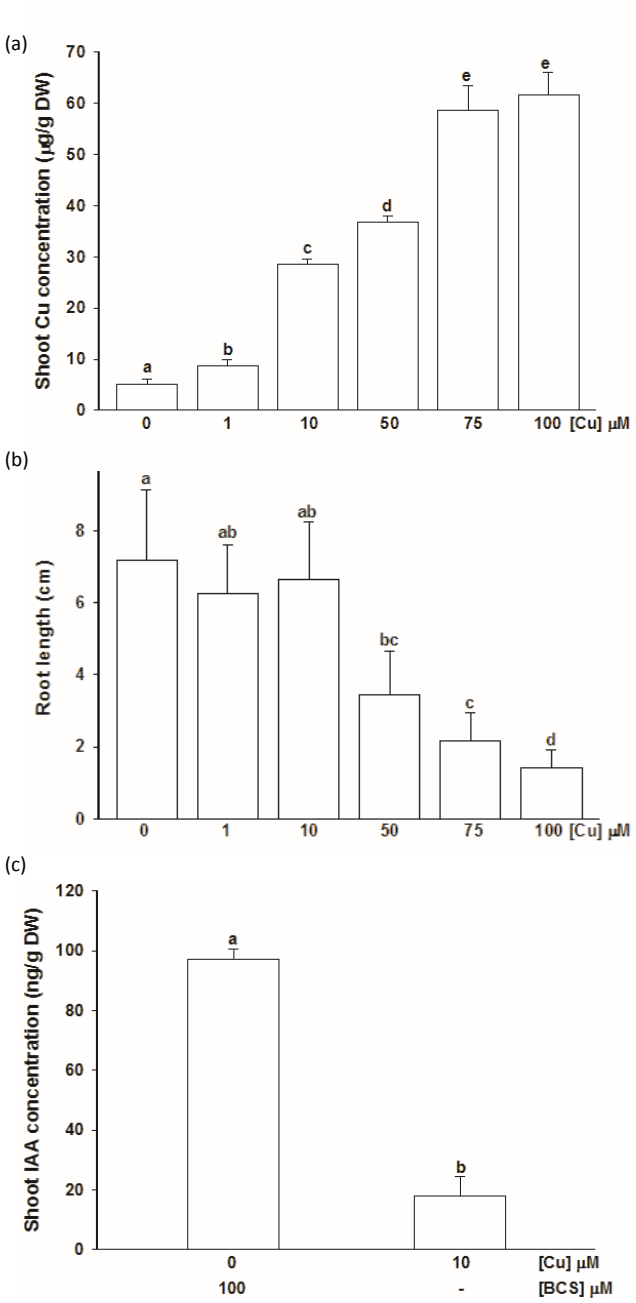

Figure 1. Characterization of *O. sativa* plants grown in media with different Cu concentrations. (a) Endogenous Cu concentration of the 8 day-old seedling shoots from the WT plants grown on a Cu scale that ranged from control conditions (0 µM $CuSO_4$) with slight Cu deficiency to severe excess (100 µM $CuSO_4$). Cu was determined by atomic absorption spectrophotometry. (b) Root length of the WT plants grown under the same conditions indicated in (a). (c) IAA concentration of WT seedlings shoots grown under severe Cu deficiency (BCS 100 µM) or Cu sufficiency (10 µM $CuSO_4$). Values are the mean±SD of n=3 replicates. The samples with a common letter are not significantly different (p-value >0.05) Kruskal-Wallis test.

Figure 1

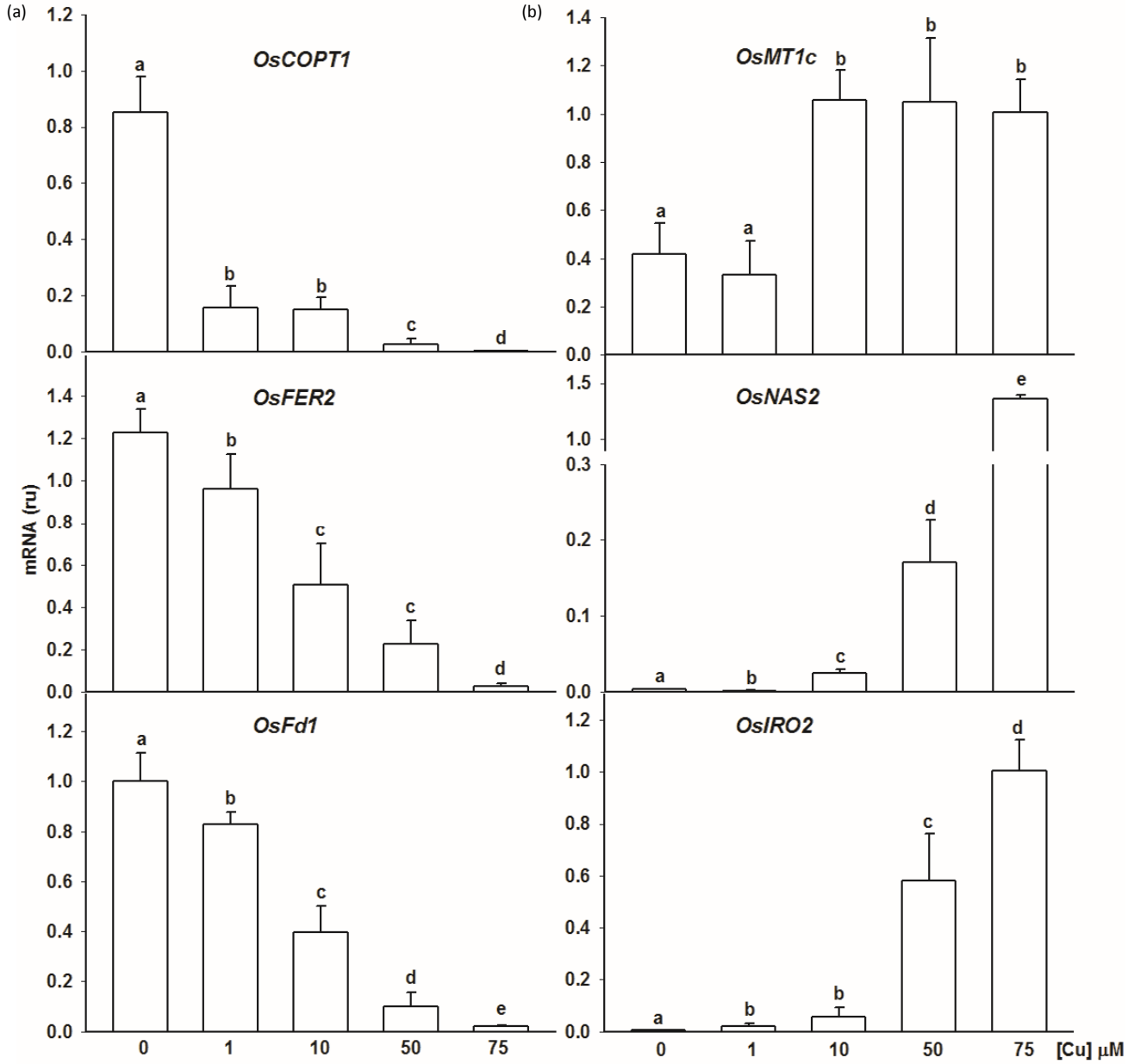

Figure 2. Expression of genes involved in metal homeostasis at different Cu contents. (a) Relative expression of the genes induced under low Cu. Expression of *OsCOPT1*, Os*FER2* and Os*Fd1* was determined by qRT-PCR from the 8 day-old WT seedling shoots grown on a Cu scale that ranged from control conditions (0 µM $CuSO_4$) with slight Cu deficiency to metal excess (75 µM $CuSO_4$). (b) Relative expression of the genes induced under Cu excess. Expression of *OsMT1c*, *OsNAS2* and *OsIRO2* under the same conditions indicated in (a). The *Actin* gene was used as a loading control. The mRNA level is expressed in relative units (ru). The values are relative to the expression level at 0 µM $CuSO_4$ in (a) and also to the expression level at 75 µM $CuSO_4$ in (b). Values are the mean±SD of n=3 replicates. Samples with a common letter are not significantly different (p-value> 0.05).

Figure 2

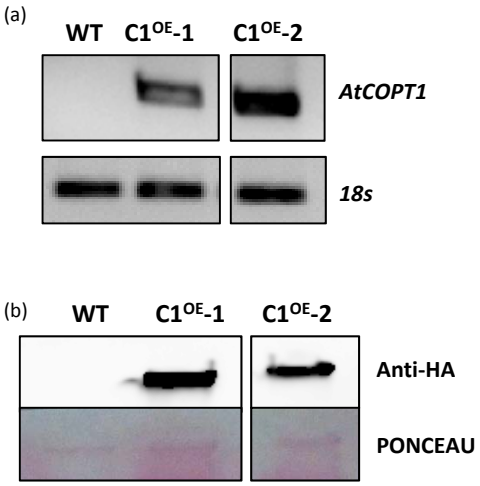

Figure 3. *AtCOPT1* expression in *O. sativa* transgenic plants. (a) *AtCOPT1* gene expression was determined by sqRT-PCR of the 8 day-old seedlings from the WT and *C1^{OE}-1* and *C1^{OE}-2* plants. The *18S* gene was used as a loading control. (b) A Western-blot analysis was used to detect the HA epitope of the seedlings from the WT and *C1^{OE}-1* and *C1^{OE}-2* plants grown under the same conditions indicated in (a). The anti-HA primary antibody labelled with peroxidase was used for Human Influenza Hemaglutinin epitope (HA) epitope detection. Ponceau staining was used as a loading control.

Figure 3

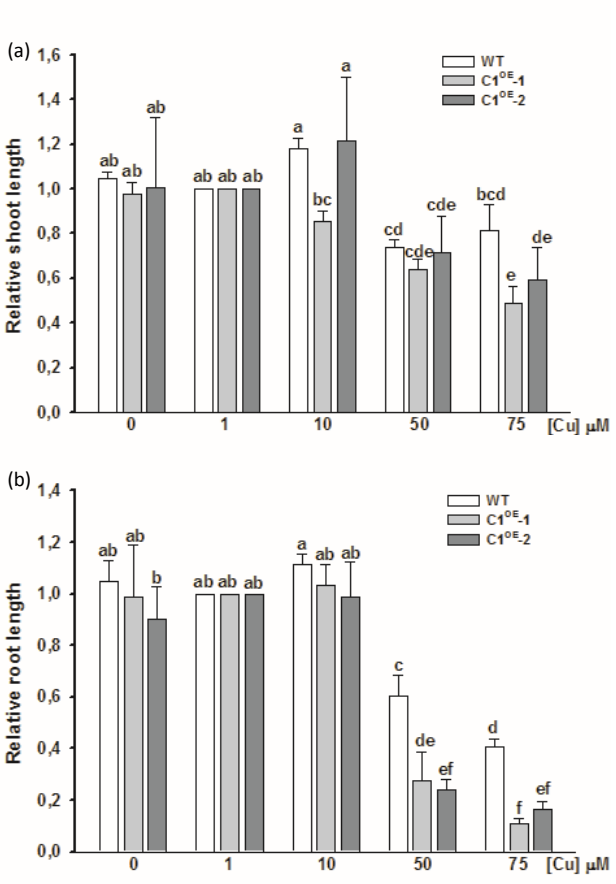

Figure 4. Length of shoots and roots of *O. sativa* WT and *C1^{OE}* plants. (a) The relative shoot length of the 8 day-old seedlings from the WT, *C1^{OE}-1* and *C1^{OE}-2* lines grown on a Cu scale that ranged from control conditions (0 µM $CuSO_4$) to Cu excess (75 µM $CuSO_4$). (b) The relative root length was measured under the same conditions indicated in (a). The ratio was calculated and normalized against each genotype sufficiency condition (1 µM $CuSO_4$). Values are the mean±SD of n=3 replicates. Samples with a common letter are not significantly different (p-value >0.05).

Figure 4

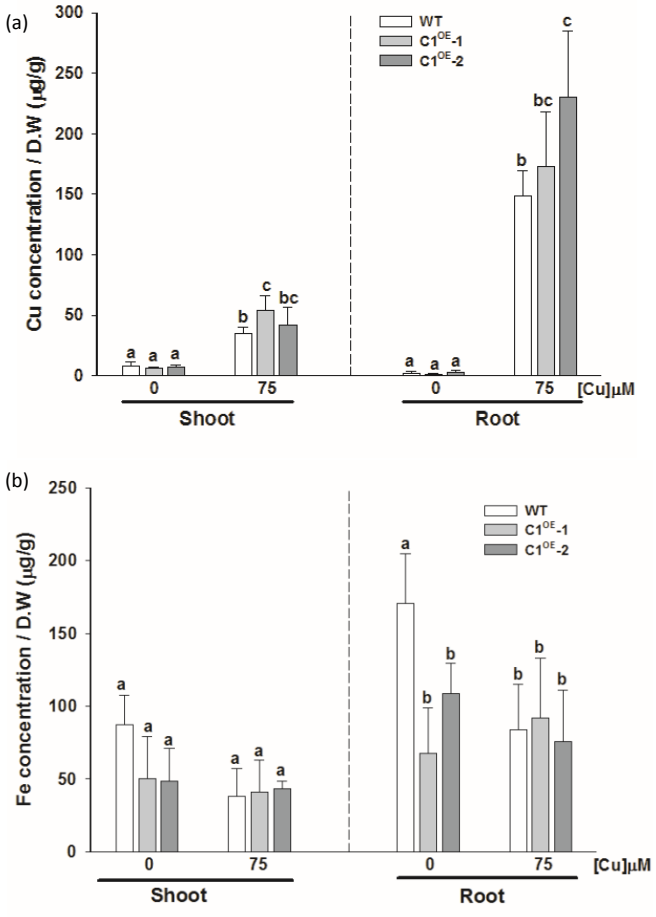

Figure 5. Metal concentration of *O. sativa C1^{OE}* plants grown in media with a different Cu status. (a) Cu concentration of the shoots and roots of the 8-day-old seedlings from the WT, *C1^{OE}-1* and *C1^{OE}-2* lines grown under control conditions (0 µM $CuSO_4$) or excess (75 µM $CuSO_4$) of Cu. (b) Fe concentration of the shoots and roots of the seedlings from WT, *C1^{OE}-1* and *C1^{OE}-2* grown under the same conditions indicated in (a). Values are the mean±SD of n=3 replicates. Samples with a common letter are not significantly different (p-value >0.05).

Figure 5

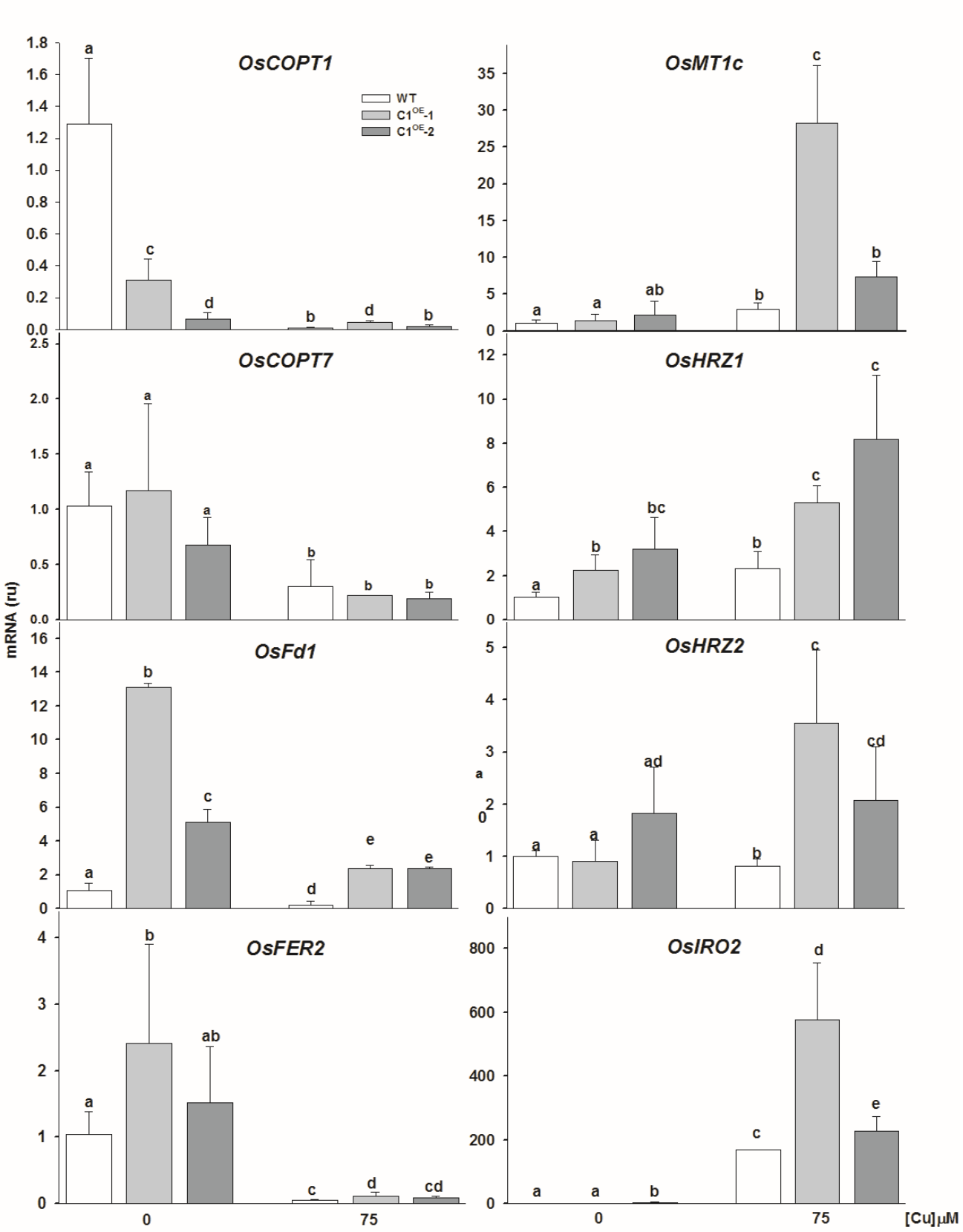

Figure 6. Relative expression of *OsCOPT1*, OsCOPT7, *OsMT1c*, *OsFd1*, *OsFER2*, *OsHRZ1*, *OsHRZ2* and *OsIRO2* genes in the WT and *AtCOPT1* overexpressing rice plants**.** Relative gene expression analyzed by qRT-PCR of the WT and *C1^{OE}* 8-day-old seedling shoots grown under control conditions (0 µM $CuSO_4$) and excess (75 µM $CuSO_4$). The *Actin* gene was used as a loading control. The mRNA level is expressed in relative units (ru). Expression values are relative to the WT seedlings grown under Cu deficiency conditions. Values are the mean±SD of n=3 replicates. Samples with a common letter are not significantly different (p-value >0.05).

Figure 6

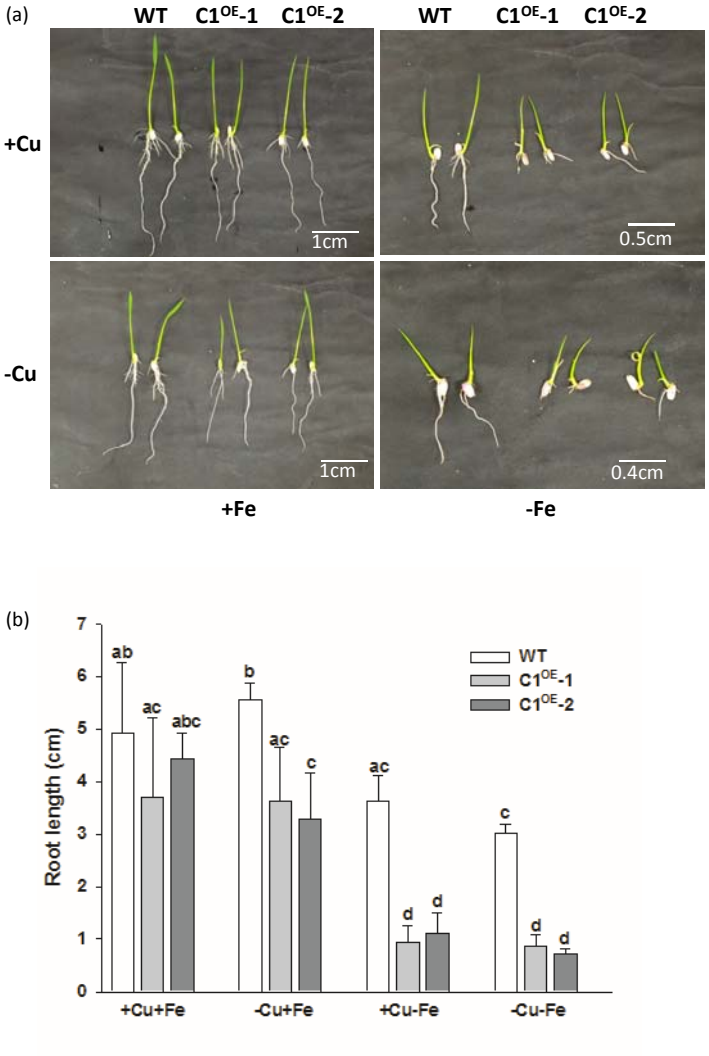

Figure 7. Characterization of the *O. sativa* $C1^{OE}$ plants grown in media with different Cu and Fe contents. (a) Representative photographs of the WT, $C1^{OE}$ *-1* and $C1^{OE}$ *-2* plants grown with different media: Cu and Fe sufficiency (+Cu+Fe), Cu deficiency (-Cu+Fe), Fe deficiency (+Cu-Fe), Cu and Fe deficiency (-Cu-Fe). (b) Root length of the 8 day-old seedlings of the WT, $C1^{OE}$ *-1* and $C1^{OE}$ *-2* plants grown under the same conditions as in (a). Represented values are the mean±SD of n=3 replicates. Samples with a common letter are not significantly different (p-value>0.05).

Figure 7

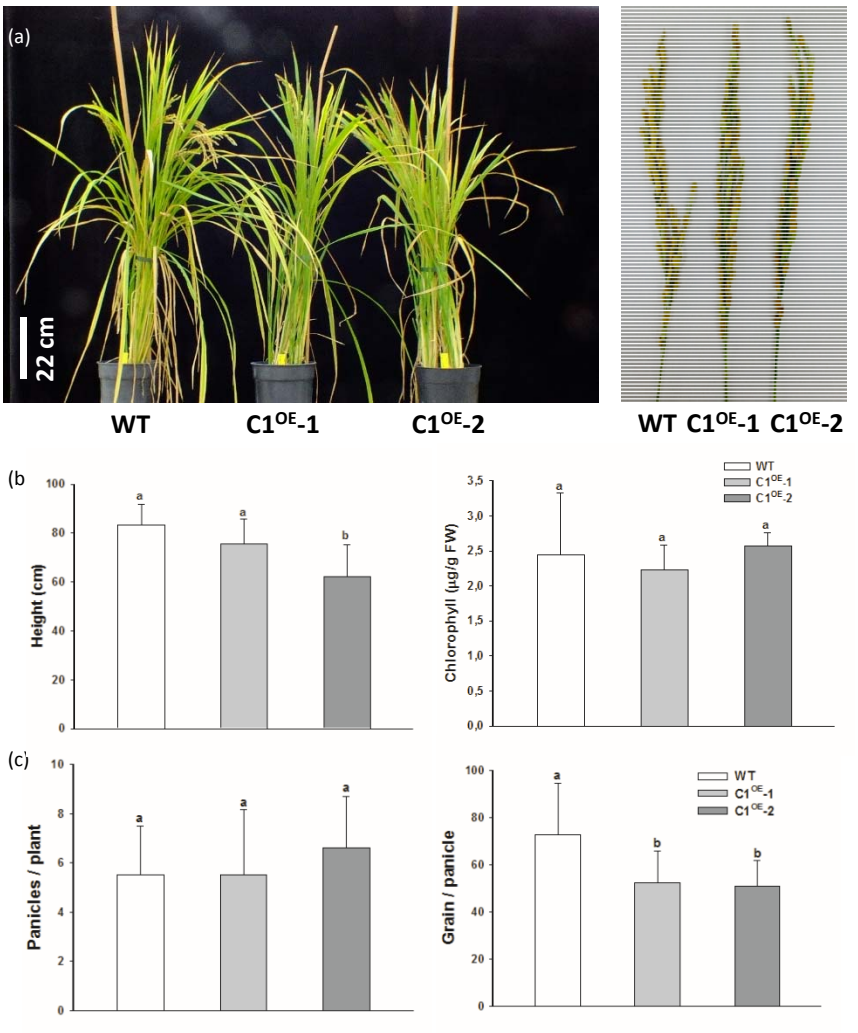

Figure 8. Characterization of the *O. sativa* $C1^{OE}$ plants grown under greenhouse conditions. (a) Representative photographs of the 5-month-old from the WT, $C1^{OE}$*-1* and $C1^{OE}$*-2* plants and panicles. (b) Plant height and leaf chlorophyll content per gram of fresh weight of the rice WT and $C1^{OE}$ plants**.** (c) Panicles per plant and grain per panicle of the WT and $C1^{OE}$ plants. Represented values are the mean±SD of n=3 replicates. Samples with a common letter are not significantly different (p-value >0.05)

Figure 8

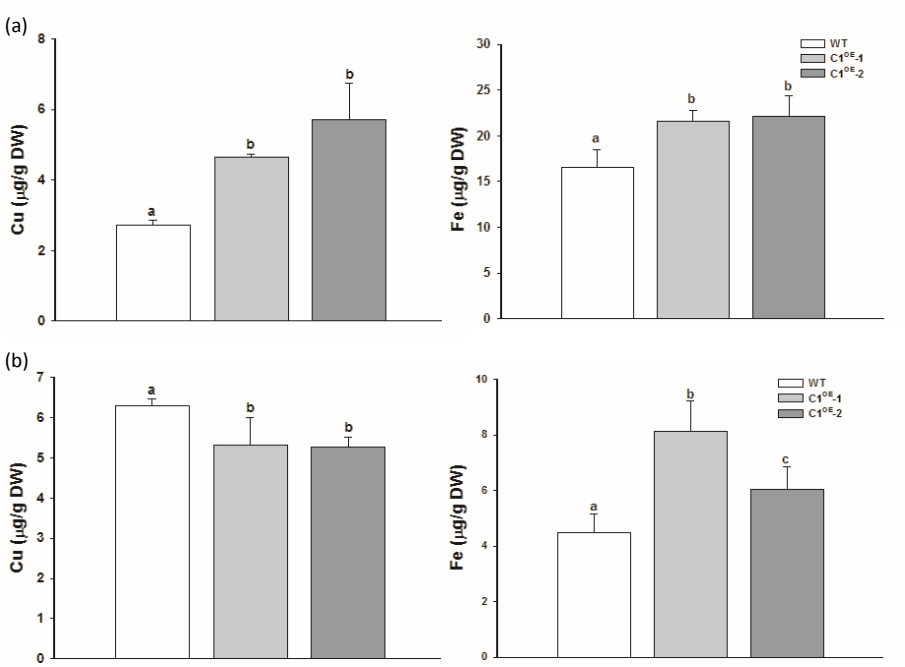

Figure 9. Metal seed concentration in the *O. sativa* $C1^{OE}$ plants grown under greenhouse conditions. (a) Cu and Fe concentrations of the brown rice grain of the WT and $C1^{OE}$ plants. (b) Cu and Fe concentrations of the white rice grain of the WT and $C1^{OE}$ plants. Represented values are the mean±SD of n=3 replicates. Samples with a common letter are not significantly different (p-value>0.05).

Figure 9

Supplemental material

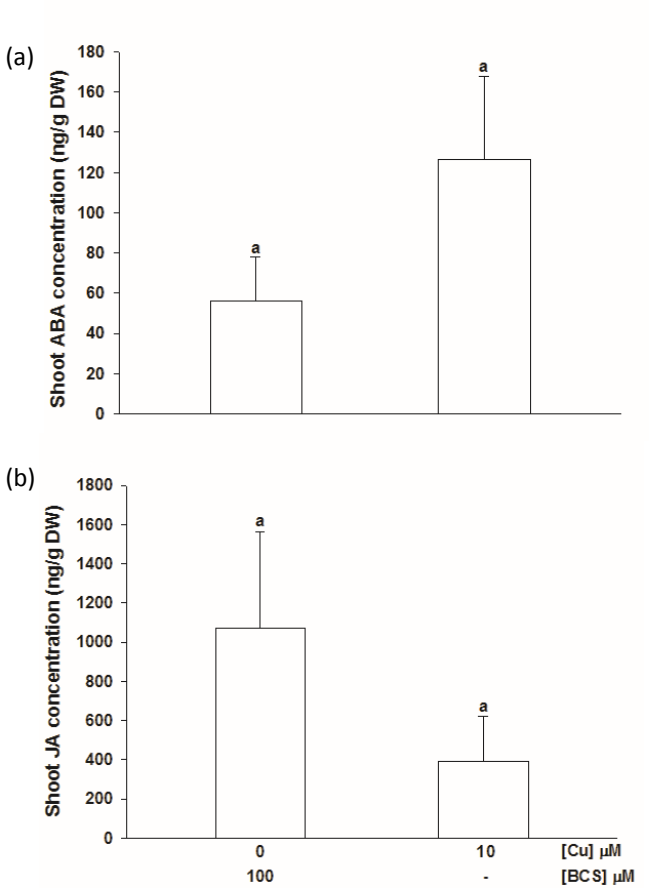

Figure S1 Hormone concentration in *O. sativa* plants. (a) Shoot ABA concentration of the 8-day-old seedlings of the WT plants grown under severe deficiency (BCS 100 µM) or sufficiency (10 µM $CuSO_4$) of Cu. (b) Shoot JA concentration of the 8-day-old seedlings of the WT plants grown under same conditions as in (a). Represented values are the mean±SD of n=3 replicates. Samples with a common letter are not significantly different (p-value >0.05).

Figure S1

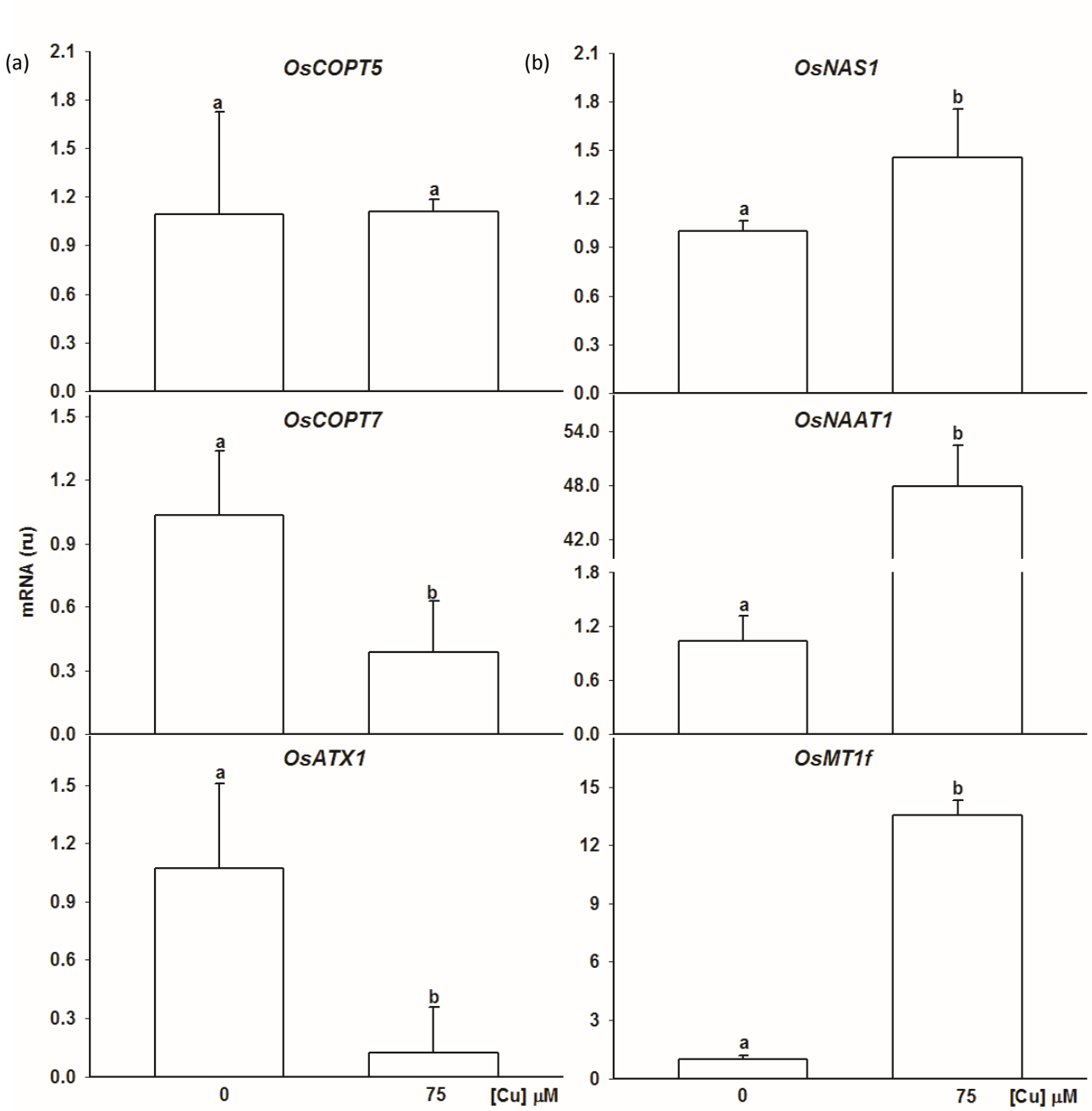

Figure S2 Gene expression in the WT plants with different Cu status. (a) Relative gene expression of *OsCOPT5*, *OsCOPT7*, *OsATX1* of the WT 8-day-old seedlings grown on control conditions (0 µM $CuSO_4$) and excess (75 µM $CuSO_4$). (b) Relative gene expression of *OsNAS1*, *NAAT1*, *OsMt1f* of the WT 8-day-old seedlings shoots grown in same conditions as in (a). Expression values are relative to the values of seedlings grown under Cu deficiency conditions. Represented values are the mean±SD of n=3 replicates. Samples with a common letter are not significantly different (p-value>0.05).

Figure S2

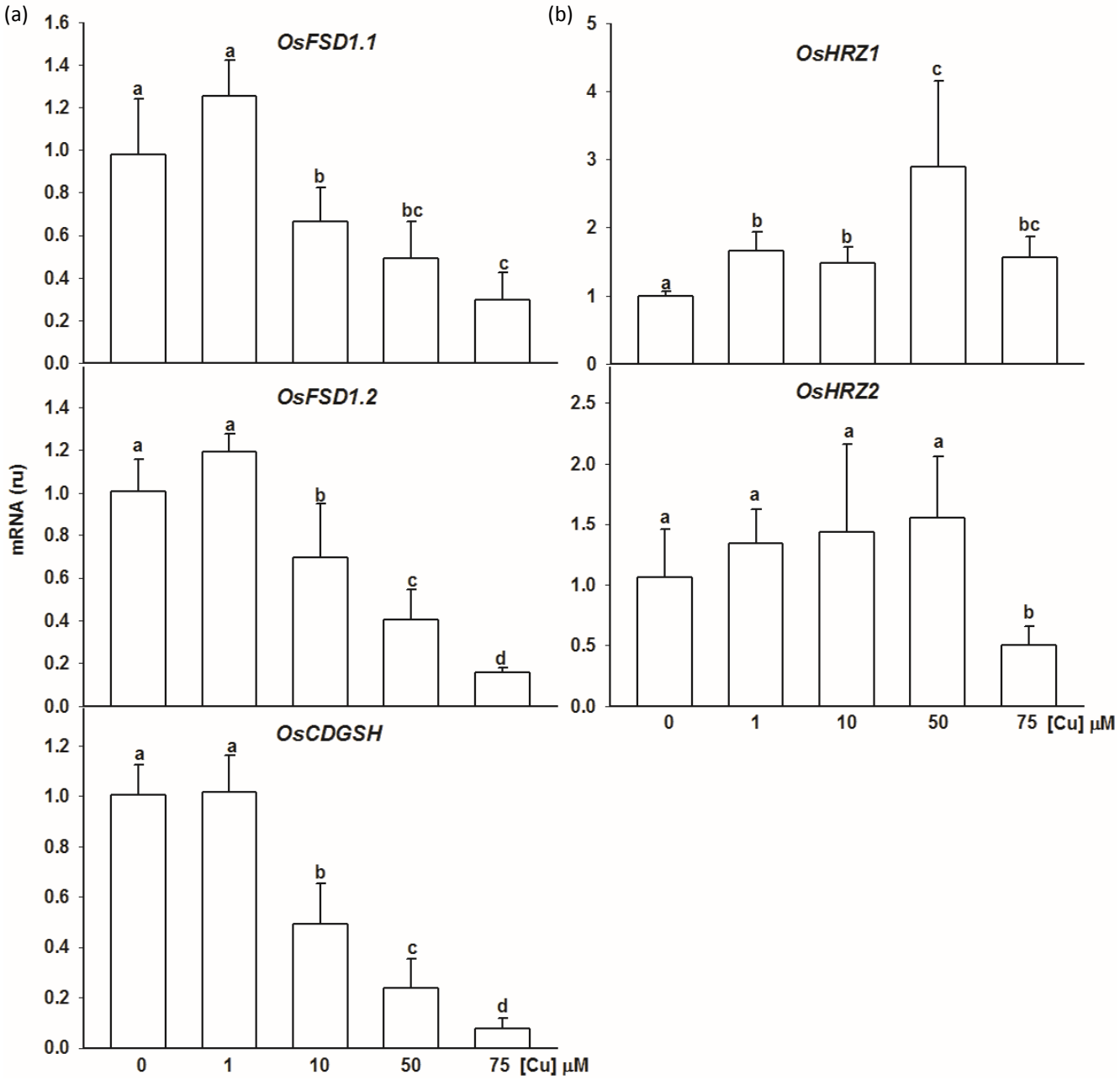

Figure S3 Gene expression in the WT plants with different Cu status. (a) Relative gene expression of *OsFSD1.1*, *OsFSD1.2*, *OsCDGSH* of the WT 8-day-old seedlings shoots grown on a Cu scale from control conditions (0 µM $CuSO_4$) to excess (75 µM $CuSO_4$). (b) Relative gene expression of *OsHRZ1* and *OsHRZ2* of the WT 8-day-old seedlings grown in same conditions as in (a). Expression values are relative to the values of seedlings grown under Cu deficiency conditions. Represented values are the mean±SD of n=3 replicates. Samples with a common letter are not significantly different (p-value>0.05).

Figure S3

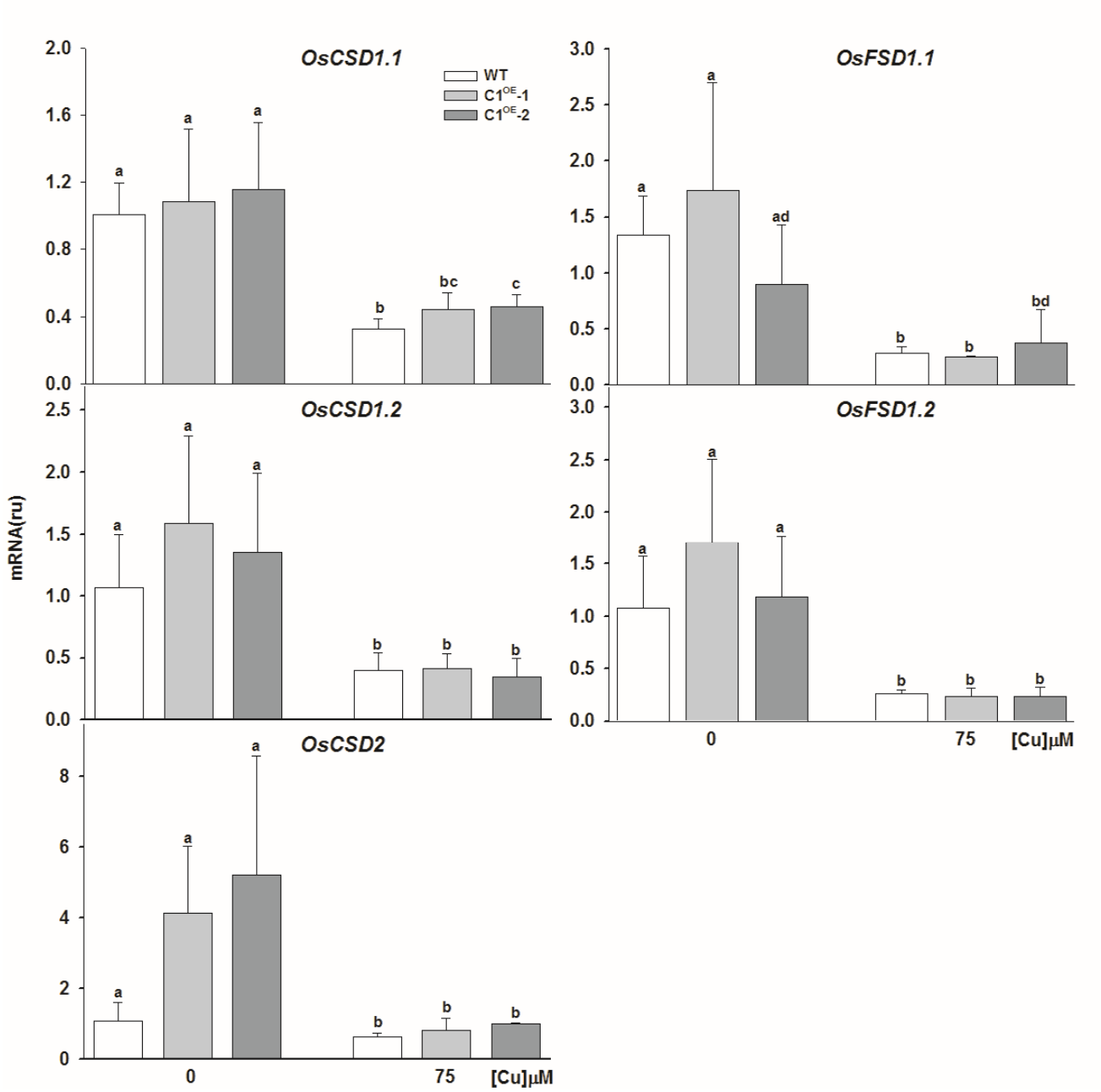

Figure S4 The SOD gene expression of the WT and *AtCOPT1* overexpressing rice plants. Relative expression of genes *OsCSD1.1*, Os*CSD1.2*, Os*CSD2* (encoding Cu, Zn SODs), *OsFSD1.1* and *OsFSD1.2* (encoding Fe SODs) of the WT and *C1*^{OE} 8-day-old seedlings shoots grown under control conditions (0 µM $CuSO_4$) and excess (75 µM $CuSO_4$). Expression values are relative to the WT seedlings grown under Cu deficiency. Represented values are the mean±SD of n=3 replicates

Figure S4

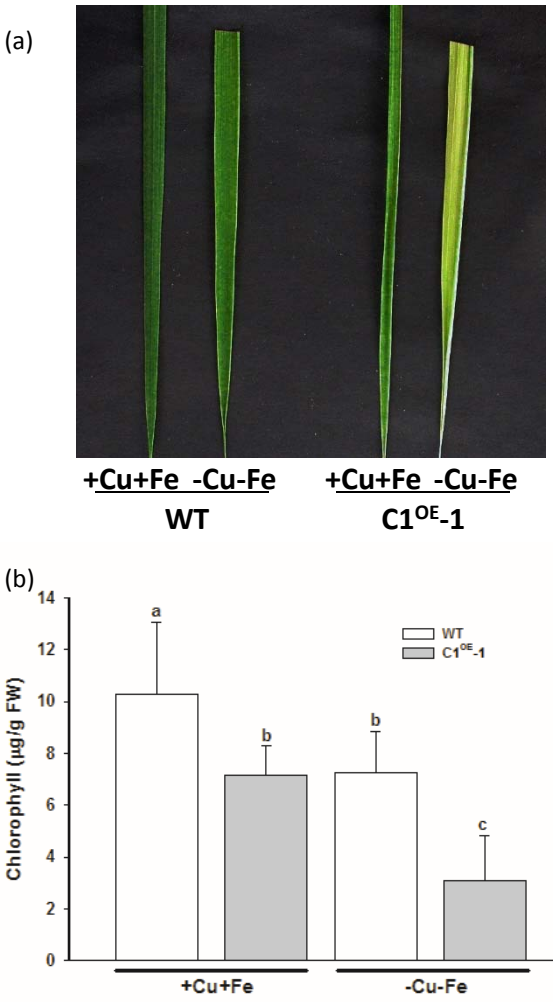

Figure S5 Characterization of the WT and *AtCOPT1* overexpressing rice plants grown in hydroponic cultures. (a) Representative photographs of 1 month-old plants. The WT and *C1^{OE}-1* plants were grown in different hydroponic cultures under different Cu and Fe conditions: Cu and Fe sufficiency (+Cu+Fe) and double Cu and Fe deficiency (-Cu-Fe). (b) Leaf chlorophyll content. Values of chlorophyll per gram of fresh weight of the WT and *C1^{OE}-1* 1 month-old plants grown under the same conditions as in (a). Represented values are the mean±SD of n=3 replicates. Samples with a common letter are not significantly different (p-value >0.05).

Figure S5

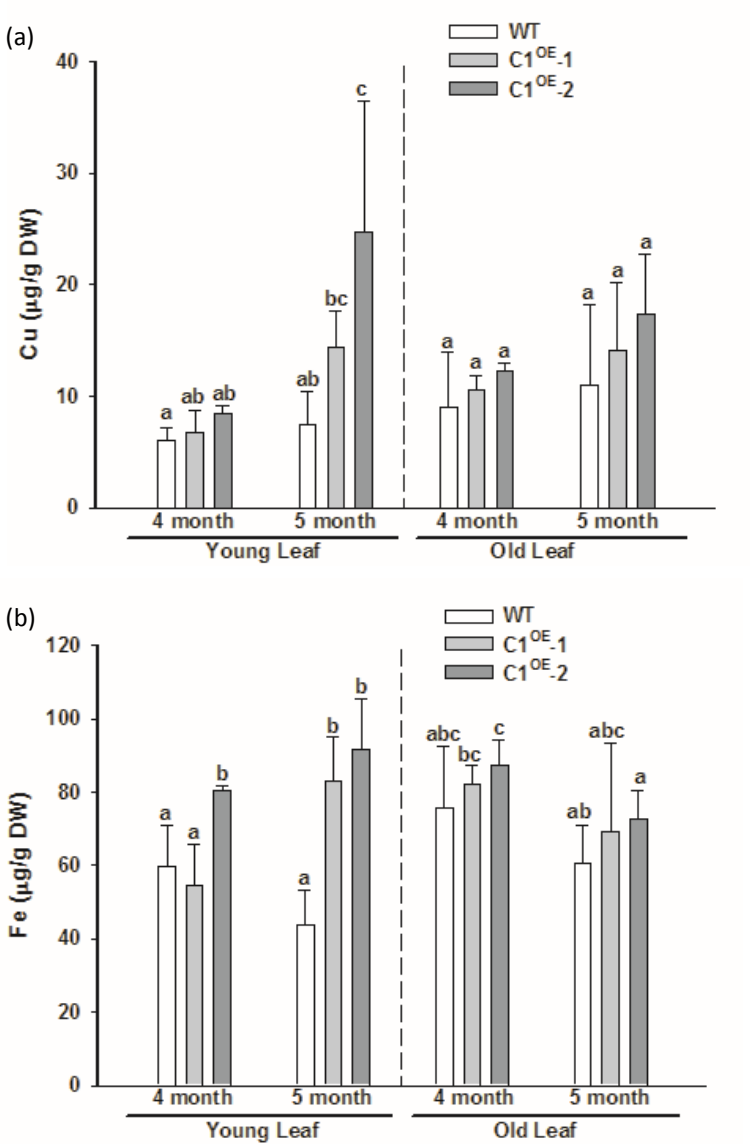

Figure S6 Metal concentration of the WT and AtCOPT1 overexpressing rice plants grown in soil. (a) Cu concentration in young and old leaves of the WT and $C1^{OE}$ from 4 and 5 month-old plants grown in soil (b) Fe concentration of the WT and $C1^{OE}$ plants grown under the same conditions as in (a). Represented values are the mean±SD of n=3 replicates. Samples with a common letter are not significantly different (p-value> 0.05).

Figure S6

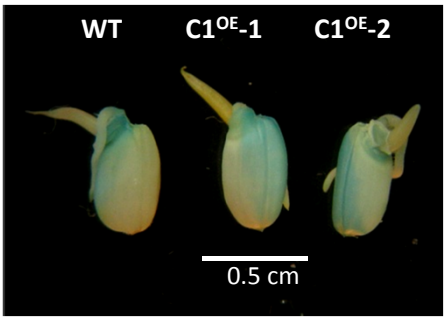

Figure S7 Perl´s staining of the brown rice grain of the WT and *C1^{OE}* plants. Seeds were germinated for 3 days in ½MS and photographed after Perl´s stained.

Figure S7

Supplemental Table SI Oligonucleotides used in RT-PCR reactions.

Gene	Sequence (5´-3´)		qPCR
	forward	reverse	Conditions
OsCOPT1	GGCGTACCTGCTCATGCT	GTCGTTCTTGCGGTCCTC	
OsCOPT5	TGCACATGACCTTCTTCTGG	CGCGAGCATGATGAGGTAT	
OsCOPT7	CTCCGCCTTCTACCAGTACC	GGCGAGCATGAGGAGGTAG	
OsFER2	CGCAGTAGCAATGGAGTGAA	CCCCAAAATACACCATCACC	
OsFd1	AGGGATCGACCTGCCTTACT	ATGAGGTCGTCCTCCTTGTG	
OsCDGSH	GGAAGGAGGAGGAGAAGGTG	CAAGTAAGGGCCCCACATTA	
OsATX1	AGTCCATGCCTCAGGTTGAT	ACCGACCTTGAGGACAACAG	
OsMT1c	CAACCCCTGCAACTGCTAAA	CACTTGGTTTTCCAGCCATAA	1 cycle 50ºC 2min
OsMT1f	TGAGAAGATCACCACCACCA	TTAGCAGTTGCAGGGGTTG	
OsNAS1	AAGGTCGGTGCCGCCGCC	TTAGACGGACAGCTCCTTGT	1 cycle 95ºC 2min
OsNAS2	GTTCCAGAAGGCGGAAGAGT	GCCTAGCATCATCCACACAA	
OsNAAT1	TTTATCCAAGGTGGCAGAGG	ATTGCTACCCAACCAAGTCG	40 cycles 95ºC-60s 60ºC-60s
Actin1	ATCCTTGTATGCTAGCGGTCGA	ATCCAACCGGAGGATAGCATG	
OsCDS1.1	GCATGTCAACTGGACCACAC	TCAGGATCAGCATGGACAAC	
OsCDS1.2	TTTGTCCAAGAGGGAGATGG	CATTTCCAAGATCACCAGCA	
OsCSD2	ATCACATGGATTTCGCAACA	GCCAGCAACAAGGCTGTTAT	
OsFSD1.1	GTCGTACAGGCAGCTTCACA	GGATTCAAACATGGACAGCA	
OsFSD1.2	ACAAAGGCAGGGCTGTAGAT	TGGGTTGCCGTTGTTGTATG	
OsHRZ1	GAATTCCACAAATGCCGGGAGAAAGG	AGCCAGCAAGGCGTCCAA	
OsHRZ2	TGAAGCTGCATTGGTCACTC	TATCAGCCGTTTGTGAGCAG	

Gene	Sequence (5´-3´)		sqPCR
	forward	reverse	Conditions
AtCOPT1	CAATGGATCCATGAACGAAGG	CCTGAGGGAGGAACATAGTTAG	30 cycles 60ºC
18S	ATGATAACTCGACGGATCGC	CTTGGATGTGGTAGCCGTTT	20 cycles 55ºC